

THE GEOLOGY OF THE FE3 OPEN-CAST, SADIOLA, MALI: STRATIGRAPHY, STRUCTURE AND INTRUSIVE ROCKS

Moshala Matabane- 0419643y

School of Geosciences

University of the Witwatersrand, Johannesburg

Geology 4000- Honours

13 October 2008

Supervisor: Prof. Kim A.A. Hein

Chamber of Mines Chair and Professor of Mining Geology

School of Geosciences

University of the Witwatersrand, Johannesburg



Declaration

I declare that this dissertation/thesis is my own work. I have correctly acknowledged all the sources, to ideas used in this dissertation/thesis. This dissertation/thesis is submitted for a Bachelor of Science degree with Honours in Geology at the University of the Witwatersrand, Johannesburg. It has not been submitted before in any other university for any examination or degree.

Signature:

Date: 13 October 2008

Acknowledgements

I would like to thank Société D'Exploitation des Mines d'Or de Sadiola S.A. (SEMODS), and Anglogold Ashanti for supporting this project financially and for providing the necessary maps and reports of the study area. Thanks to the staff at the Sadiola mine for sharing their resources with us during the field work.

Thanks to my supervisor, Prof. Kim Hein for taking time to teach where I did not understand and for motivating me during the completion of the project. Thanks for your patience, insightful comments and encouragement.

I would like to thank Mr Mamadou Diarra for his patience and kindness during the fieldwork. Thanks for the great assistance you provided me and my supervisor.

Thanks to Mr Mario Pratas for providing field equipment I needed to complete the field work of the project. Thanks for your generosity.

I would like to thank my colleagues, Mr Asinne Tshibubudze and Mr Bjinse Dankert. Your constructive comments and patience during the completion of the project added more value to the project.

Thanks to my family and friends for supporting me and encouraging me to take the project.

Abstract

The FE3 open casts (Sadiola goldfield, Mali) are operated by the Société d'Exploitation des Mines d'Or de Sadiola S.A.. The open casts comprise meta-sedimentary rocks that can be divided into five units; lower slump facies, upper slump facies, siltstone-greywacke unit, greywacke unit and a laterite profile. The lower slump facies consists of siltstone beds and is characterised by massive chaotic slump folds and olistoliths. The upper slump facies consists of greywacke-siltstone beds and is characterised by turbidite beds, slump folds and fluid escape structures. The siltstone-greywacke unit is characterised by turbidite beds. The greywacke unit is carbonaceous.

The sediments of the lower slump facies, upper slump facies and the siltstone-greywacke unit are interpreted to have been deposited in a seismically-active turbulent environment, with mass transport and debris flow along a delta-front. The greywacke unit is interpreted to represent a significant change in the depositional environment, from a slump dominant pro-delta to shallow marine setting.

The sedimentary units are crosscut by granodiorite dykes. The granodiorite dykes are form part of the Sekokoto pluton (granodiorite-tonalite). The sedimentary units have been contact metamorphosed around the granodiorite dykes.

Primary hydrothermal gold mineralisation occurs in the contact aureole around the dykes in the lower slump facies, and in breccia zones and quartz-arsenopyrite veins that crosscut the sedimentary units. The primary gold mineralisation is associated with hydrothermal chlorite-sericite alteration which is related to hydrothermal fluids that are interpreted to have originated from the granodiorite dykes. Secondary placer gold mineralisation occur in palaeochannels that cross-cut the sedimentary units and the primary gold mineralisation. The placer gold mineralisation is interpreted to have been derived from erosion of the primary hydrothermal mineralisation.

Table of Contents

Contents	Pages
Declaration	2
Acknowledgements	3
Abstract	4
1. Introduction	
1.1. Preamble	7
1.2 Location and Physiography	7
1.3 Aims and objectives	8
2. Regional Geology	
2.1 Preamble	10
2.2 Basement rocks	11
2.3 Mako Supergroup	11
2.4 Dialé-Dalemé Supergroup	11
2.5 Falemé volcanic belt	11
2.6 Kofi Series	11
2.7 Intrusive rocks	12
2.8 Metamorphism	12
2.9 Regional structure	12
2.10 Gold metallogeny in West Africa	13
3. Methodology	
3.1 Data Collection	19
4. Results	
4.1 Lithologies	20
4.1.1 Lower Slump facies	20
4.1.2 Upper slump facies	20
4.1.3 Siltstone-greywacke sequence	21
4.1.4 Greywacke	21
4.1.5 Laterite profile	21
4.2 Granodiorite dykes	22

4.3 Structure	22
4.4 Petrography	22
4.4 Gold Mineralisation	23
5. Discussion	
5.1 Depositional Environment	37
5.2 Gold bearing breccias and veins	40
5.3 Placer gold mineralization	41
5.4 Geological history	41
6. Conclusion	44
References	45
Appendix: Petrography	

Chapter 1: Introduction

1.1 Preamble

The FE3 open cast is situated in the Sadiola goldfield in Mali. The goldfield also includes the giant Sadiola and FE4 open casts which are mined by the Société d'Exploitation des Mines d'Or de Sadiola S.A., and is a Joint Venture partnership between AngloGold Ashanti, IAMGOLD, the Malian Government and the IFC. Gold production at Sadiola goldfield began in mid-1997: the FE3 open cast is currently in the feasibility stages.

The geology and metallogenic setting of the FE3 open cast has not been investigated, mapped or researched to date. Therefore the relationship between the stratigraphy, structures and intrusive rocks is not known, but it is considered by Sadiola mine geology team to be important in determining the tectonic setting and the timing of gold mineralization in the goldfield.

Therefore the main objective of this study is to describe the stratigraphy, structure and intrusive rocks that occur in the goldfield. Also the tectonic setting and the relative timing of gold mineralization will be determined. Determining the relative timing of gold mineralization will assist in predicting the occurrence of gold in new exploration projects in the Sadiola area.

1.2 Location and physiography

The FE3 open cast is located in the Sadiola area in Mali, West Africa. The Sadiola goldfield is located 80 km west of the capital city of Bamako on the western border of Senegal and Mali (Fig. 1). Mali is a landlocked, Sahel country and is mostly semi-desert or desert. The climate ranges from sub-tropical in the south to arid in the north. The country is mostly dry, but in the south of the country, and at the Sadiola goldfield, 4-5 months of rainy season significantly affects mining operations. December and January are the driest and coldest months of the year with zero rainfall, and temperature ranging from 16°C to 33°C.

The field component of this study took place in January 2008 before the rainy season started and temperatures peaked. During the dry season a dry, dust-laden harmattan haze is common and this reduces visibility.

Mali's official language is French but African languages are widely used; 80% of population speaks Bambara. The majority of Mali's population is Muslim. A small percentage of the population practice indigenous religion and Christianity.

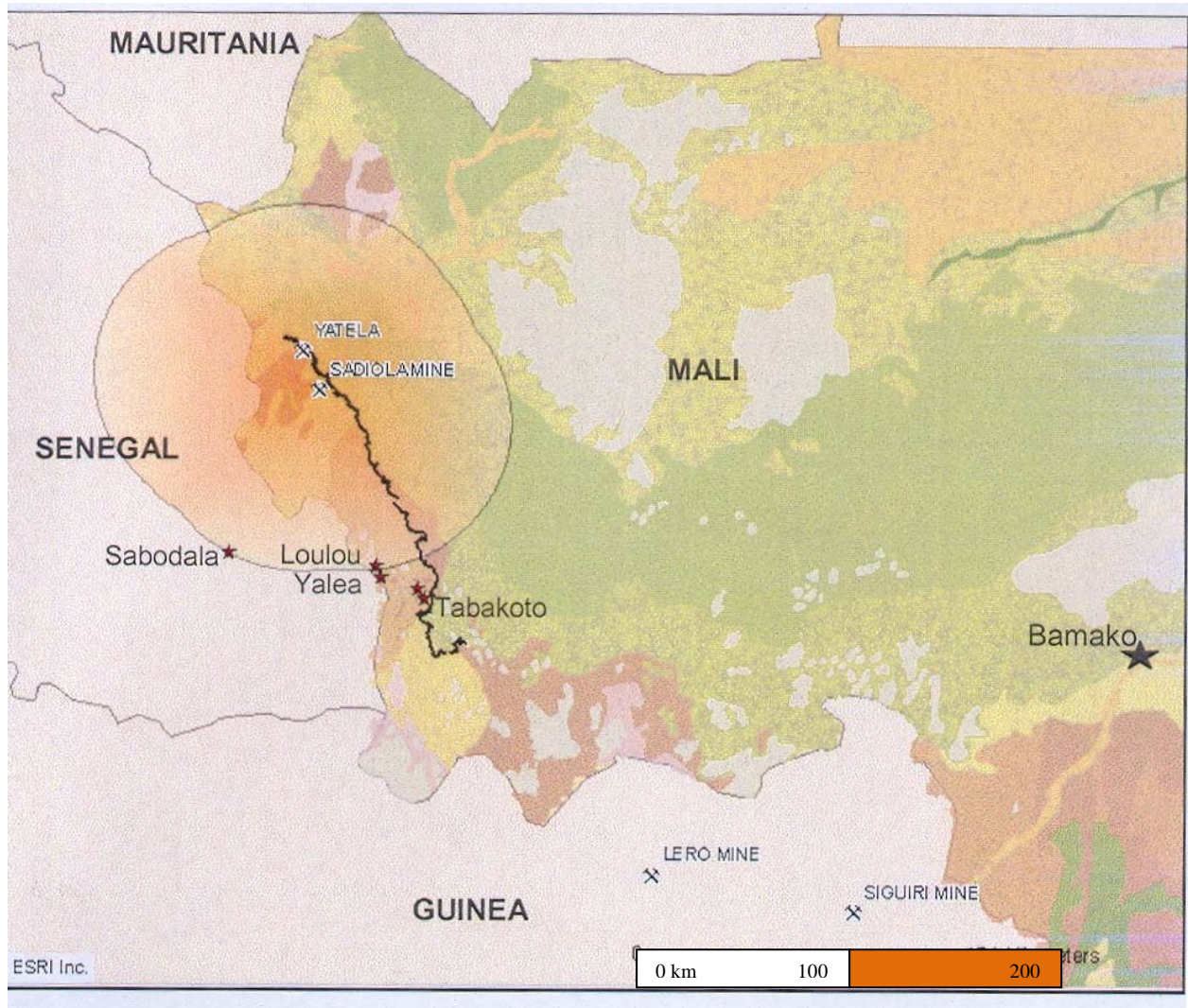
Malaria and other arthropod-borne diseases prevail in Mali and high rates of children suffer from malnutrition. Mali is very poor and one of the poorest countries in the world.

Mining is a significant component to Mali's economy and accounted for 26% of gross domestic product (GDP) in 2005, with gold mining accounting for 80% of mining activity (US Department of State, 2008).

1.3 Aims and objectives

The main objective of the project is to define the stratigraphy in the study area by subdividing the facies successions. Furthermore, detailed mapping of structures (if present) will be done with the purpose of determining the relative timing of structural events. Another objective of the project will be mapping of the intrusive bodies and determining their relationship to stratigraphy and structure. The timing of gold metallogenesis and processes that led to gold formation will be investigated.

Figure1: Locality map of Sadiola goldfield (modified from Robins, 2006).



Legend

~~~~~ : Escarpment

★ mines

☒ mines

## **Chapter 2: Regional geology**

### **2.1 Preamble**

The West African craton has been divided into four major domains; the Reguibat Rise, the Leo-Man Rise, the Kayes Inlier and the Kéniéba Inlier (Liégeois et al., 1991; Thiéblemont et al., 2004; Dioh et al., 2006) (Fig. 2). The domains are separated by the Taoudenit basin which is Phanerozoic in age (Dioh et al., 2006). The Reguibat and the Leo-Man domains consist of an Archaean terrain in the west and a Palaeoproterozoic terrain in the east (Egal et al., 2002; Gueye et al., 2008). The Kéniéba and the Kayes Inliers are Palaeoproterozoic terrains (Liégeois et al., 1991) and the study area is situated in the Kéniéba Inlier in Mali.

The Kéniéba Inlier has been divided into the Mako Supergroup, the Dialé-Dalemé Supergroup, Falemé volcanic belt and the Kofi Series (Hirdes et al., 2002) (Fig. 3). The Kéniéba Inlier is a Birimian terrain that was accreted during the Eburnean Orogeny at 2.2-2.0 Ga (Liégeois et al., 1991; Taylor et al., 1992; Gueye et al., 2008). The Eburnean Orogeny in the Kéniéba Inlier is characterized by the emplacement of calc-alkaline granitoids which intruded the volcanic and sedimentary sequences of the inlier (Leube et al., 1990; Dioh et al., 2006). The post-Eburnean Senegalo-Malian graben lies east of the Senegalo-Mali Shear Zone and trends N-S (Hirdes et al., 2002). The Kofi Series overlies the graben in Mali; the series has not been dated.

The stratigraphic succession of the Kéniéba Inlier is listed in Table 1. The Birimian rocks of the Kéniéba Inlier unconformably overlie the Sandikounda Amphibolite-Gneiss (SAG) basement (Dia et al., 1997). The basement consists of dioritic to tonalitic rocks aged at  $2194 \pm 6$  (Dia et al., 1997, Pb-Pb age; Pawlig et al., 2006, T<sub>DM</sub> Sm-Nd). The oldest Birimian rocks of the inlier are tholeiitic basalts and andesites of the Mako Supergroup, which unconformably overlie the SAG basement. These volcanic sequences are dated at  $2195 \pm 11$  Ma (Dia et al., 1997; detrital zircons, Pb-Pb age) and at  $2063 \pm 41$  Ma (Abouchami, 1990; Sm-Nd). The Mako Supergroup is overlain by the Dialé-Dalemé Supergroup which consists of Birimian sequences dated at  $2096 \pm 8$  Ma (Ledru et al., 1991; Pb-zircon evaporation; Hirdes et al., 2002). The Dialé-Dalemé Supergroup is overlain by the Falemé volcanic belt which is dated at  $2099 \pm 4$  Ma (Hirdes et al., 2002; Pb-Pb age). The Kofi Series, which outcrops only in Mali, overlies the volcanic belt and has not been dated (Dioh et al., 2006).

The sequences are intruded by Eburnean granitoids aged at  $2045 \pm 27$  to  $1973 \pm 33$  Ma (Ledru et al., 1991; Taylor et al., 1992; Pb-Pb; Pawlig et al., 2006). The post-Eburnean age Senegalo-Mali graben is located between the Falemé volcanic belt and Kofi Series and is

interpreted to have formed during activation on the Senegalo-Mali Shear Zone (Bassot et al., 1986 in Pawlig et al., 2006).

## 2.2 Basement rocks

The Sandikounda Amphibolite Gneiss Complex (SAG Complex) forms the basement to the Mako Supergroup. It consists of two major components; Banded Gneiss and the Sonfarara unit (Gueye et al., 2008). The Banded Gneiss consists of heterogeneous associations of diorite to tonalite, while the Sonfarara unit comprises amphibolite that has been interpreted as xenoliths (approx. 500m in diameter) with a metamorphic ‘compositional banding’ (Dia et al., 1997; Pawlig et al. 2006; Gueye et al., 2008).

## 2.3 Mako Supergroup

The Mako Supergroup is predominantly composed of tholeiitic pillowved basalt and calc-alkaline andesite. These meta-volcanic rocks are inter-layered with immature meta-sedimentary and meta-volcaniclastic rocks (Hirdes et al., 2002; Dioh et al., 2006).

## 2.4 Dialé-Dalemé Supergroup

The Dialé-Dalemé Supergroup is composed of meta-sedimentary sequences inter-bedded with calc-alkaline volcanics (Pawlig et al., 2006). The meta-sedimentary sequences consist of intercalations of carbonate, volcaniclastic, siliciclastic and turbiditic units (Schwartz et al., 2004). The volcanic sequences consist of andesite lavas, with rhyolitic pyroclastites (Schwartz et al., 2004; Dioh et al., 2006).

## 2.5 Falemé volcanic belt

The Falemé volcanic belt is poorly exposed and extensively latteritised throughout the Kéniéba Inlier. Hirdes et al. (2002) concluded that andesite and felsic lava dominate the belt, but volcaniclastic units, chemical sediments (e.g., chert and manganiferous shale) and meta-greywacke also occur throughout the volcanic belt. Hirdes et al. (2002) interpreted these sequences as proximal volcanic rocks. The Falemé volcanic belt is associated with major skarn-type iron deposits (Schwartz et al., 2004).

## 2.6 Kofi Series

The Kofi Series crops out east of the Senegalo-Mali Shear Zone and is sinistrally displaced (Hirdes et al., 2002). The series consists of Birimian-type basin sediments, and includes orogenic-type metasediments and volcaniclastic sequences. The series is crosscut by numerous tourmaline-rich quartz veins which host gold mineralisation in the Loulo goldfield (Fig. 1) southeast of the study area (Fouillac et al., 1993).

## 2.7 Intrusive rocks

The Birimian sequences of the Kéniéba Inlier are intruded by calc-alkaline granitoids (TTG suite) that were emplaced during the Eburnean Orogeny at 2200-2000 Ma (Leube et al., 1990; Eisenlohr et al., 1991; Hirdes et al., 2002). Two major magmatic events have been identified in the Kéniéba Inlier; at 2.16-2.11 Ga and at 2.08-2.07 Ga (Gueye et al., 2008). The early magmatic event resulted in the emplacement of the Badon-Kakadian batholith; then later resulted in the emplacement of the late granitoids of the Saraya batholith (Gueye et al., 2008).

The 120 km long Badon-Kakadian batholith intrudes the Mako Supergroup and consists of numerous TTG suite plutons and a layered plutonic complex (Dioh et al., 2006). The complex is composed of werhlite, pyroxenite, gabbro and diorite (Gueye et al., 2008). The batholith also hosts granitoids that are dated at  $2199 \pm 68$  Ma (Bassot and Caen-Vachette, 1984 in Ledru et al., 1991; Rb-Sr whole rock; Gueye et al., 2008).

The Saraya batholith intrudes the Dialé-Dalemé Supergroup and includes the Balangouma and Boboti plutons (Hirdes et al., 2002). The Saraya batholith is composed of biotite-bearing tonalite to granite, while the Boboti and Balangoma plutons comprise gabbro to amphibole-biotite bearing monzogranite (Dioh et al., 2006) that are dated at  $1973 \pm 33$  Ma (Ledru et al., 1991; Rb-Sr). The Falemé volcanic belt is intruded by Na-rich, belt-type granitoids (Dioh et al., 2006).

## 2.8 Metamorphism

During the Eburnean Orogeny, the Birimian meta-volcanic and meta-sedimentary sequences of the Kéniéba Inlier were subjected to regional metamorphism to greenschist facies (Liégeois et al., 1991; Taylor et al., 1992; Debat et al., 2003). The contact aureole of granitoids are characterised by staurolite-sillimanite-garnet mineral assemblages indicating that metamorphism reached amphibolite facies in grade (Debat et al., 2003; Pawlig et al., 2006). Peak metamorphic conditions reached  $500\text{-}600$  °C and 4-6 kbar and has been dated at approximately 2.1 Ga, which falls in the time interval of the Eburnean Orogeny (Hirdes et al., 2002; Pawlig et al., 2006, U-Pb age on sphene).

## 2.9 Regional Structure

The rocks of the Kéniéba Inlier were deformed during the Eburnean Orogeny at 2.1 Ga (Milési et al., 1992). Two major strike-slip shear zones dominate the Inlier; the Senegalo-Malian Shear Zone and the Main Transcurrent Zone (Ledru et al., 1991) (Fig. 4). Ledru et al.

(1991) reported four phases of structural evolution; an extensional phase during the deposition of Birimian sequences, a compressional phase (referred to as D1), an Eburnean compressional tectonic phase and a late extensional phase. The early Birimian and the extensional phase are marked by the deposition of clastic sediments, intense hydrothermal activity, and emplacement of tholeiitic lavas and dykes. These lavas and dykes are interpreted to indicate a period of extensional tectonism during their emplacement (Milési et al., 1989 in Ledru et al., 1991). This resulted in the formation of the Lower Birimian sequences.

A compressional phase (D1) affected the lower Birimian sequences and indicates a fairly high crustal level tectonic activity with tendency towards thrusting (Ledru et al., 1991).

The Eburnean orogeny followed extension and accompanied the formation of major sinistral strike-slip shear zones and the emplacement of granite bodies (Ledru et al., 1991). There are two hypothesis proposed for the Eburnean tectonics; 1. a general NW-SE crustal shortening with associated strike-slip faulting, and 2. transcurrent deformation (Lemoine et al., 1990; Milési et al., 1992; Watkins et al., 1993; Pons et al., 1995; Dioh et al., 2006) . The hypothesis of transcurrent deformation has been generally accepted and the major shear zones are assumed to have been active over a period of 50 million years as there is evidence of sinistral strike-slip faults in the oldest intrusions of the Kéniéba Inlier (Ledru et al., 1991). Subsequent strike-slip shearing was initiated along fractures formed during the late extensional phase.

## 2.10 Gold metallogeny in West Africa

West African gold production has a long history. In the 16<sup>th</sup> century, the Gold Coast of West Africa accounted for 35% of the entire world's gold production although gold production had decreased significantly since that time (Béziat et al., 2008). Major gold deposits occur in Ghana, Burkina Faso and Mali. The Ghanaian gold province is the largest in West Africa and is considered a world-class gold deposit region (Komla, 1993). Ghana and Mali are currently the second and third largest gold producers in Africa, respectively (Middleton, 2007).

Three types of primary deposit have been distinguished in West Africa; pre-orogenic stratiform deposits; syn-orogenic deposits; late-orogenic discordant mesothermal gold mineralization (Milési et al., 1992). Pre-orogenic stratiform deposits have been reported in the Loulo district of Mali, which hosts tourmalinised turbidite. The deposits are associated with earlier extensional zones (Fouillac et al., 1993; Béziat et al., 2008) and occur predominantly within Lower Birimian sequences. Syn-orogenic deposits include gold

mineralization in disseminated sulphides in volcanic and plutonic rocks and gold mineralization in conglomerate beds (Milési et al., 1992). These types of deposits have been reported in Burkina Faso (Diénémera), Ghana (Tarkwa district), Mali (Syama), and Ivory Coast (Yaouré-Angovia) (Milési et al., 1992; Feybesse et al., 2006). Syn-orogenic deposits are related to brecciated hydrothermal zones.

Late orogenic discordant mesothermal gold mineralisation includes gold-arsenopyrite lode mineralization and quartz lode mineralization with native gold and poly-metallic sulphides (Béziat et al., 2008). Discordant mesothermal mineralization (auriferous arsenopyrite and Au-bearing quartz vein lodes) are reported in Ghana (Ashanti, Pretea, Marlu, Bogosu, Konongo), Ivory Coast (Asupiri and Anuiri) and Mali (Sanoukou district) (Milési et al., 1992). Gold mineralization occurs within NE-trending tectonic corridors that are several kilometres long (Ledru et al., 1988 in Milési et al., 1992; Feybesse et al., 2006).

Quartz lode mineralization with poly-metallic sulphides is interpreted to have formed during the last brittle to brittle-ductile stages of the Eburnean Orogeny (Béziat et al., 2008). This type of deposits has been reported in Mali (Kalanga), Guinea (Banora), Burkina Faso (Poura), Senegal (Sabodala) and Ivory Coast (Hiré) (Milési et al., 1992). Gold-bearing arsenopyrite lode mineralization predates quartz lode mineralization, but they are locally superimposed.

**Table I: Stratigraphic succession of the Kéniéba Inlier.**

| <b>Supergroup</b>       | <b>Dominant rock types</b>                                                                                                                              |
|-------------------------|---------------------------------------------------------------------------------------------------------------------------------------------------------|
| Kofi Series             | (undated)<br>Orogenic-type metasediments and volcaniclastic sequences                                                                                   |
| Falémé volcanic belt    | 2099±4 Ma (Pb-Pb age; Hirdes et al. (2002))<br>Volcanoclastics and chemical sediments                                                                   |
| Diale-Dalema Supergroup | 2096±8 Ma (Pb-zircon; Ledru et al., 1991)<br>Consists of detrital sediments and calc-alkaline volcanics. Intruded by the Saraya pluton                  |
| Mako Supergroup         | 2063±41 Ma (Abouchami, 1990; Sm-Nd)<br>2195±11 Ma (Dia et al., 1997; Pb-Pb)<br>Tholeiitic pillowed basalts and alkaline andesites with immature basalts |
| Basement                | Sandikounda Amphibolite Gneiss Complex<br>2194±6 Ma (Pawlig et al., 2006, Sm-Nd; Dia et al., 1997, Pb-Pb)                                               |

**Figure 2: Simplified Geology of the West African craton (modified after Dioh et al., 2006).**

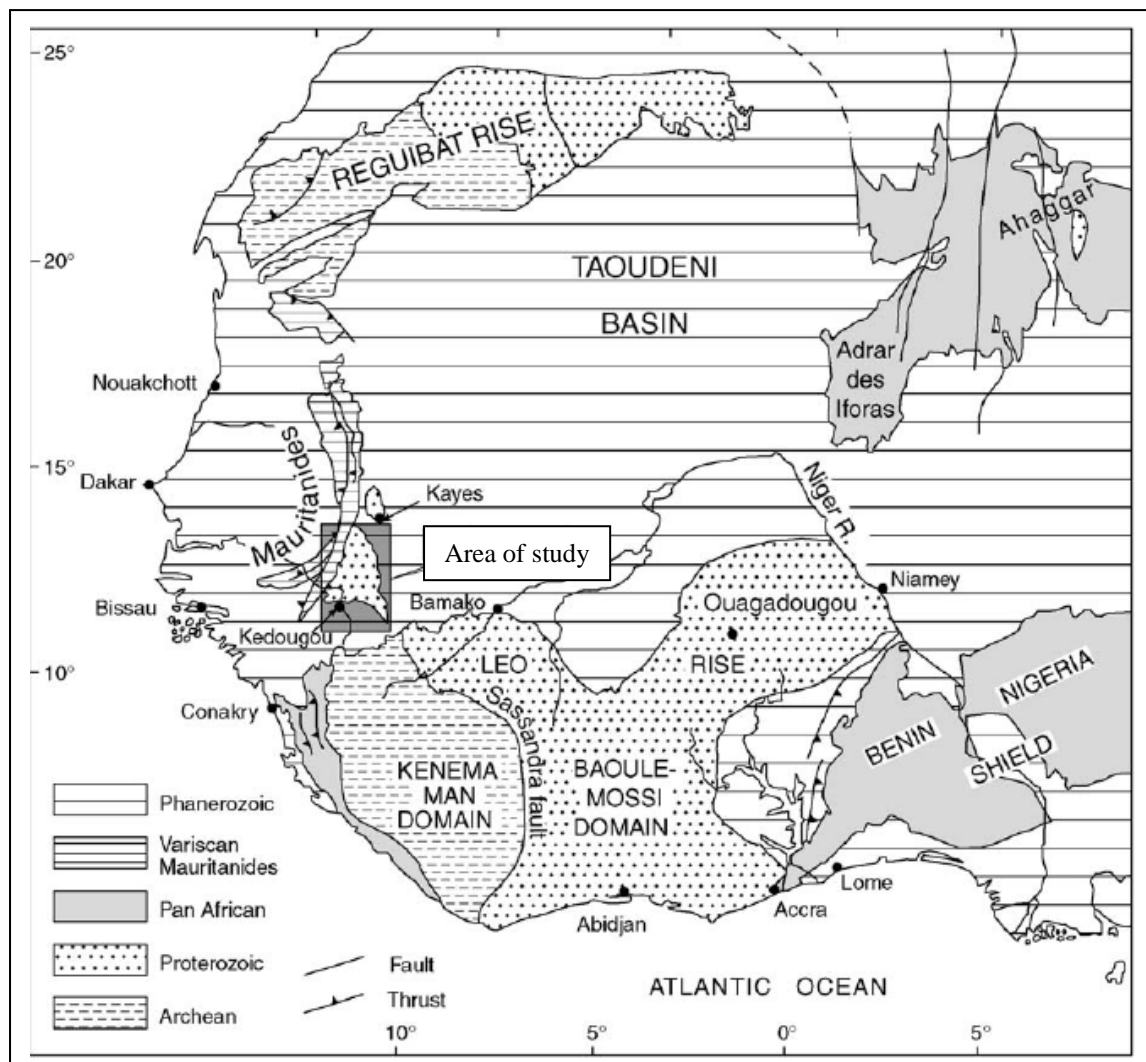


**Figure 3: Simplified geology of the Kéniéba Inlier (Dioh et al., 2006)**

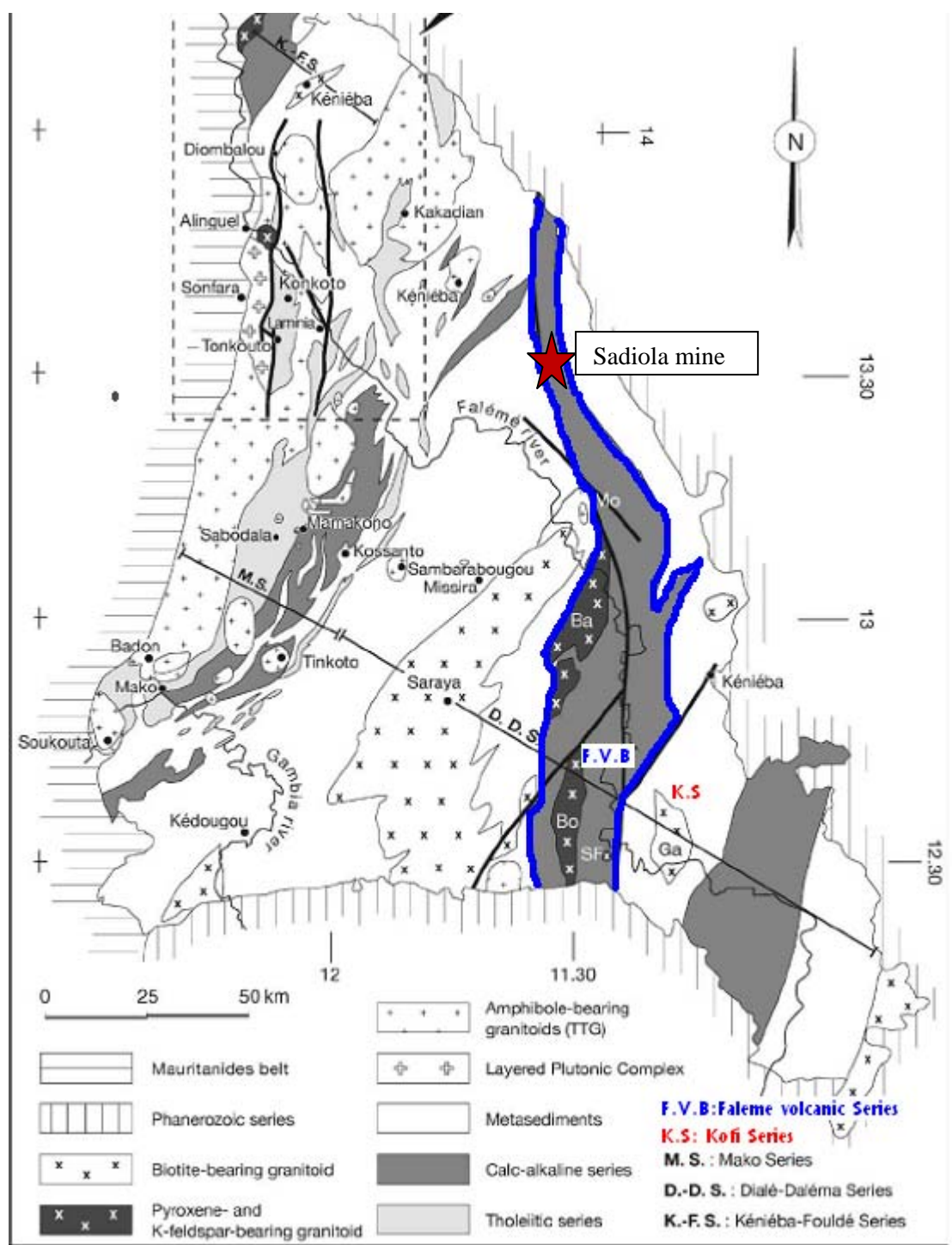
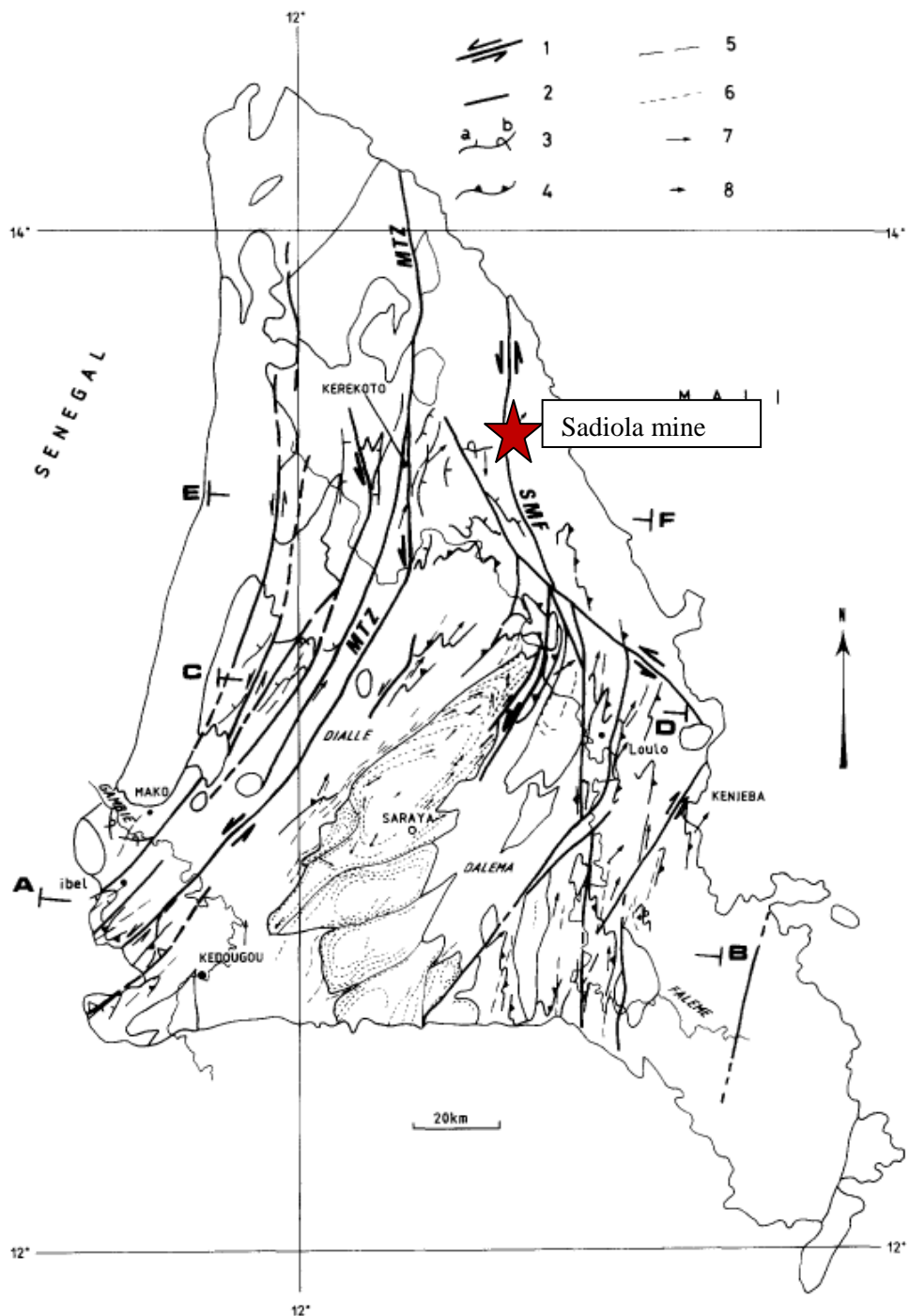


**Figure 4: Structural map of the Kéniéba Inlier (modified after Ledru et al., 1991).**

1 = transcurrent fault; 2 = reverse fault; 3 = trace of stratificationin B2 (a=normal position, b=reverse position); 4=trace of schistosity 1 in Bl; 5=trace of schistosity 2; 6=planarfabric in the granites; 7=stretching lineation; 8=linear fabric in the granites; MTZ=Main Transcurrent Zone; SMF= Senegalese-Malian Fault.



## **Chapter 3: Methodology**

### **3.1 Data collection**

Field mapping of the FE3 open casts was completed in January 2008. At each station point, the facies were mapped, lithological data was recorded and the GPS coordinates were established. Also, where appropriate a photographic record was made and samples were collected for petrographic studies.

The data was captured using a northern hemisphere compass clinometer, and the geographic coordinates were recorded using a Garmin GPS. The GPS station data used UTM coordination system, WGS 84 datum. The point data was transferred onto mine maps. The mine maps were converted from mine grid coordinates to UTM coordinates by measuring fixed points in the field and then transferring the data onto base maps. A hand-lens was used for mineral identification in the field.

Stratigraphic facies were subdivided and the lithologies within the facies were recorded. Facing direction was determined using primary sedimentary features such as, scour and fill, cross-bedding, and turbidite sequences. Also, the orientation of the structures was measured. The contacts and contact aureole of the intrusive rocks were measured. Core-logs were completed at the mine site.

Appropriate locations in the field and selected drill-core, were sampled. The samples were labelled, bagged and then sent by air freight to the university. At the university the samples were catalogued and sent to the SGS laboratories in Boysen, Johannesburg for lapidary. These thin sections were studied under refracted light and reflected light microscopy.

## **Chapter 4: Results**

### **4.1 Lithologies**

The lithologies of the FE3 opencasts (FE3\_1, FE3\_2 and FE3\_3) are composed of sedimentary rocks. The rocks can be divided into four major units; lower slump facies, an upper slump facies, a siltstone-greywacke and a greywacke unit (Table 2). They are unconformably overlain by a laterite profile which is a result of post-Palaeoproterozoic weathering processes.

The rocks of the FE3 opencast are deformed, which resulted in the development of breccia lodes (cataclasite). The units have been intruded by granodiorite dykes. The intrusions have contact metamorphosed the rocks with the development of a contact metamorphic aureole. Gold mineralisation in the breccia lodes and in the upper slump facies consists of arsenopyrite-pyrite-gold assemblages.

#### **4.1.1 Lower slump facies**

The lower slump facies is the lowermost unit of the study area (Map 2 and 3). It is predominantly composed of siltstone, with bedding trending south at a dip of 10°E. The lower slump facies is characterised by turbidite sequences and slump folds (Figs. 5 and 6, respectively).

The lower slump facies is carbonaceous and slump structures are not massive. There are no greywacke beds in the lower slump facies. Slump features such as glide surfaces, chaotic folding and detached units are observed in the lower slump facies.

Boulders and cobbles of marble, up to 10m and 50cms in diameter, respectively are embedded in the lower slump facies. Towards the north of FE3\_2 open cast (Map 2), the marble boulders are generally massive, but in some places bedding is preserved. The boulders consist of recrystallised calcite grains but silicification is indicated from crosscutting quartz veins (Fig. 7). The marble boulders contain sulphides of pyrite and arsenopyrite (Fig. 8).

#### **4.1.2 Upper slump facies**

The upper slump facies unconformably overlies the lower slump facies, and it is characterised by slump folds and turbidites sequences. The upper slump facies consists of mudstone, siltstone and greywacke beds. The greywacke beds in the upper slump facies are

dominant in FE3\_pit 1 and consist of angular grains of quartz embedded in a fine grained matrix. The clasts range in size from less than 0.1 mm to about 5mm diameter. In the FE3\_pit 2 (Map 2), siltstone and mudstone beds with slump folds are dominant. The upper slump facies is Fe-rich and has been oxidised. Mudstone dykes are common. The mudstone dykes are typically 1cm thick and up to 20 cm long (Fig. 9). The upper slump facies consists of glide surfaces (Fig. 10) and chaotically orientated open to isoclinal to box, recumbent, overturned or upright folds with various slump fold axes orientations. In places the facies is rich in carbonate and graphite. Stratigraphic facing direction is toward the NE as indicated from turbidite beds, fining-upwards, and scour and fill. In general the trend of bedding is SE and dip 65°NE.

Primary features observed in the study area associated with the slump structures include; massive sandy sheets, floating clasts, rolled units, inverse grading and mudstone dykes.

#### 4.1.1 Siltstone-greywacke unit

The siltstone-greywacke sequence overlies the upper slump facies. Facing has been determined from primary depositional features such as scour and fill, Bouma sequences (Fig. 11) and cross bedding. Facing is generally toward the NE throughout the opencasts. The unit is bedded; beds trend SE with an average dip of 20°NE. Towards the north, in FE3\_pit 1 there is a cleavage trending NE with an average dip of 35°E.

The unit is characterised by numerous turbidite beds. Each bed consists of a lower massive sand layer with an erosional surface marked by mud clasts. The sand layer is overlain by fining-upward layers ranging from siltstone to shale. The layers have a thickness of approximately 3cm.

#### 4.1.5 Greywacke unit

The greywacke unit unconformably overlies the upper slump facies. The unit is cross-bedded. The unit is carbonate-bearing and has been metamorphosed to greenschist facies. Bedding trends to the north-west with a dip of 34° E. The greywacke consists of angular grains of quartz embedded in a finer grained quartz-chlorite-sericite matrix. Stratigraphic facing is to the East.

#### 4.1.6 Laterite profile

A laterite profile covers the study area to a thickness of more than 2 metres. Laterite is an iron-crust profile formed in humid tropical regions with contrasting seasons (Brown et al., 1994). During the wet season iron is leached from overlying soils and incorporated into

minerals at depth, and during the dry season precipitation is intensified by lack of moisture (Brown et al., 1994). The laterite profile in the study area consists of goethite and hematite aggregates.

#### **4.2. Granodiorite dykes**

NE-trending granodiorite dykes intrude the sedimentary sequences. They consist of 30% and 25% euhedral grains of microcline and orthoclase, respectively. Other minerals include, quartz (15%), plagioclase (25%), biotite (<1%) and sericite (4%). The quartz and plagioclase crystals are subhedral while biotite grains are anhedral. The granodiorite is medium-crystalline and extensively altered (Fig. 12). In places the dykes have been heavily weathered leaving a potassium-feldspar-rich residue. The dykes are interpreted to connect with the Sekokoto pluton (Fig. 13), at depth because the pluton underlies the Sadiola goldfield (Hein and Tshibubudze, 2007a) as determined from aeromagnetic data of the Kenieba Inlier (north sun angle).

The granodiorite dykes have been extensively altered. The most prominent type of alteration is sericitic alteration where crystals of plagioclase, quartz and orthoclase are replaced by sericite around the crystal boundary (Fig. 14). Another common alteration in the rocks is a deuterian alteration.

#### **4.3 Structure**

The rock units have undergone two phases of deformation. The first deformation event is mostly localised in the siltstone-greywacke unit. This is a deformation phase and indicated by a weak shear trending NE with a dip of 60°E.

The second deformation phase is a regional extensional phase. The deformation event resulted in the formation of the main structures in the study area. The main structures in the FE3 open cast are NW-trending zones of brecciation bounded by faults (Maps 1, 2 and 3). The zones consist of faults breccias and cataclasite with an average thickness of 40m. The breccia consists of clasts of calcite embedded in an iron-oxide matrix (fig. 15). The calcite clasts are angular in shape and have varying sizes from a few mm's up to 1m. The breccias zones host gold mineralisation.

#### **4.4 Petrography**

Twenty three polished thin sections were studied using reflected and transmitted light microscope. The results of the study for each thin section are outlined in the appendices.

Most of the rock samples including quartzites and marble have been recrystallised and metamorphosed. Quartz grains in the greywacke unit host stylolitic micro-textures and granoblastic quartz grains (fig. 16). These textures are interpreted to indicate deformation in the rocks. The quartzite has a pinkish potassium feldspar staining. The potassium staining is interpreted as an indication of a contact aureole around the rocks. The quartzite is very fine grained.

The marble boulders that occur in the lower slump facies contain pyritohedra (Fig. 8). These are particularly interesting as they differ in shape and origin from the ‘normal’ hexagonal pyrite. The pyrite grains of this morphology are formed in alkaline polysulphide solutions and the development of octahedral surfaces are a result of slow rate of pyritization and crystallisation in the presence of excess  $\text{CaSO}_4$  (Graham and Ohmoto, 1994).

The marble is very fine grained and completely composed of calcite. Quartz veins crosscut the calcite host rock. Sulphide-rich “micro-veins” cross-cut the host rock and the quartz veins (Fig. 7). Also the marble contains grains of microcline (Fig. 17). The microcline grains are replaced by the calcite crystal, and this is shown by the jagged edges and the calcite grains embedded in microcline.

The siltstone-greywacke, lower slump facies, upper slump facies and breccias zones host scorodite. Scorodite is an alteration product of arsenopyrite, which is formed under acidic, oxidising conditions (Verplanck et al., 2008). Arsenopyrite in the study area is associated with gold mineralisation. In the study area, arsenopyrite has been altered to scorodite.

The granodiorite is composed of plagioclase, biotite, sericite, orthoclase, quartz, and microcline. The plagioclase is subhedral, orthoclase is euhedral, microcline and quartz are subhedral and the biotite is anhedral. Sericite is an alteration mineral. The granodiorite has been deuterically altered (Fig. 12) and sericitised (Fig. 14). The granodiorite is medium-crystalline. It consists of 35% microcline, 20% plagioclase, 20% orthoclase, 20% quartz, 3% sericite and 2% biotite.

#### **4.5 Gold Mineralisation**

There are two phases of mineralisation in the study area;

1. Primary hydrothermal mineralisation
2. Secondary placer gold mineralisation

The primary gold mineralisation occurs in the breccia zones, the lower slump facies and also in breccia lodes. The secondary mineralisation occurs in palaeochannels.

The primary gold mineralisation in the breccia zones occurs in the iron oxide matrix around the calcite clasts. In the lower slump facies, the gold mineralisation is hosted by the turbidite sequences. Gold is associated with sulphides such as arsenopyrite, pyrrhotite and pyrite. The mineralised zones occur in the contact aureole of the granodiorite dykes and are associated with hydrothermal alteration.

Relatively high concentrations of gold are found at the base of palaeochannels in the study area. The base of the palaeochannels is marked by an unconformity (Fig. 18). The drainage patterns and the morphology of the palaeochannels are controlled by the presence of weak zones such as joints and fractures. The palaeochannels are also developed along the structural breccias zones. Relatively smaller palaeochannels occur NE of the FE3 opencasts and these palaeochannels drain into a relatively large palaeo-river system in FE3\_pit 3 (refer to Map 1, 2 and 3). The drainage system in the south occurs along a wider breccias zone which implies that the development of the drainage system is favoured by weaker zones in the rocks.

The base of these palaeochannels has high water content and the mine has an active dewatering program. This has implications for mining and hydrogeology such as excess drainage of water into the mining changes in groundwater movement and storage.

**Table 2: Stratigraphic succession of the FE3 open cast.**

| Lithologies              | Description                                                            |
|--------------------------|------------------------------------------------------------------------|
| Laterite                 | weathering profile                                                     |
| Greywacke                | metamorphosed; bedded                                                  |
| Siltstone-greywacke unit | foliated; bedded                                                       |
| Upper Slump facies       | siltstone-greywacke beds; massive slump folds; fluid-escape structures |
| Lower Slump facies       | siltstone beds; mineralised; slump folds                               |

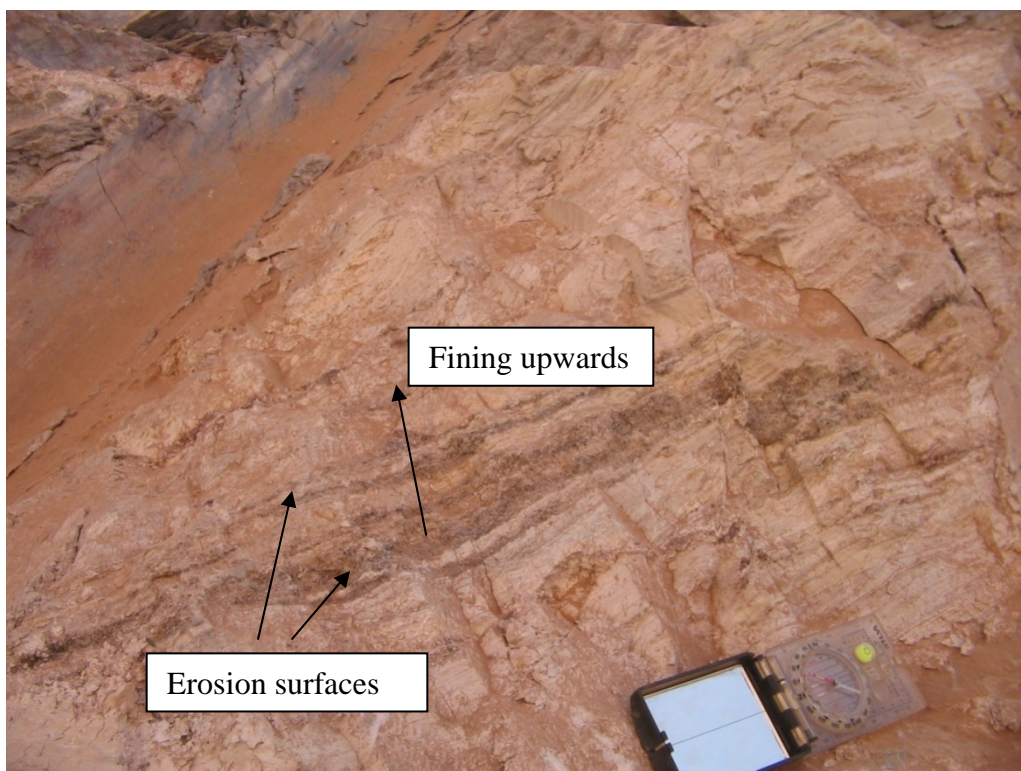


**Fig. 5: Turbidite sequences of the lower slump facies. Location: FE3-pit 2; GPS= 1536162; 0216258**



**Fig. 6: Slump folds and soft sediment deformation in the lower slump facies. Location: FE3-pit 2; GPS= 1534765; 0216396.**

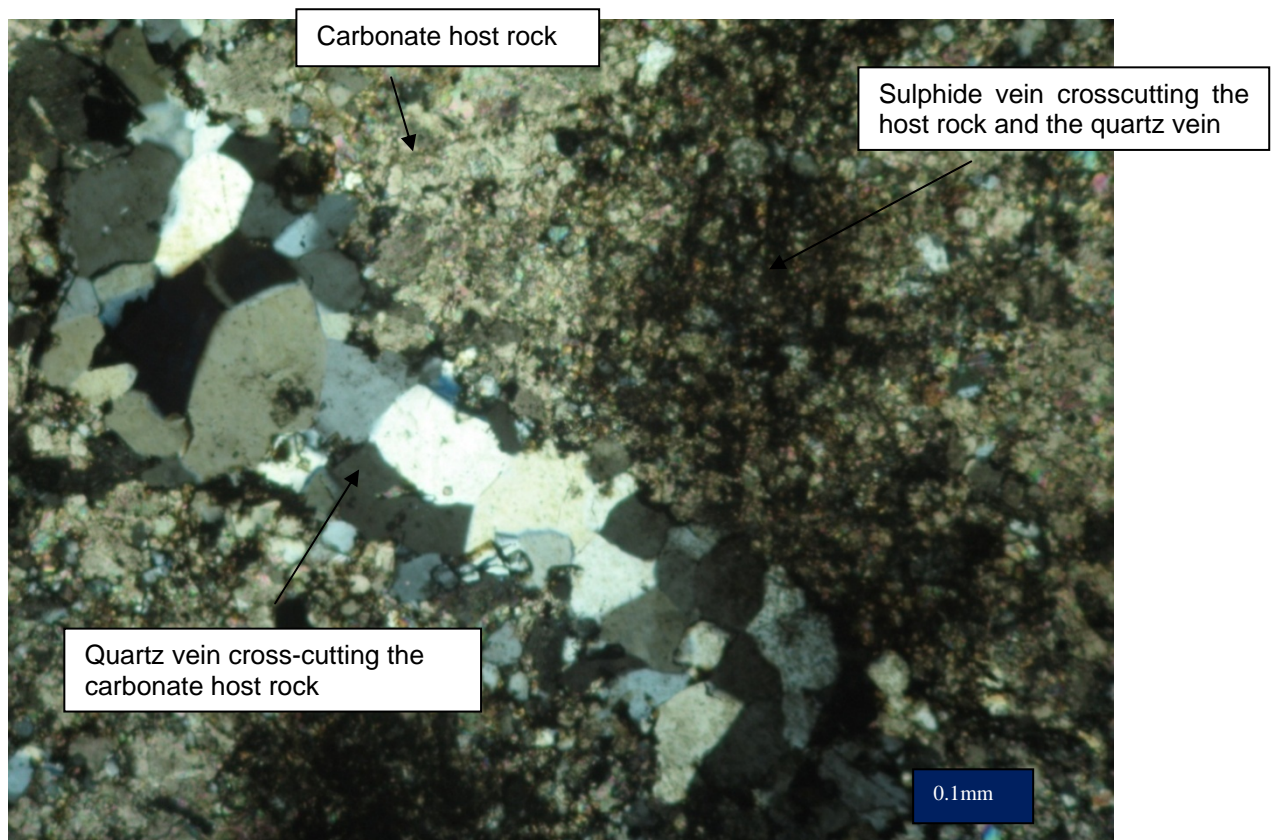


**Fig. 7: Quartz vein and sulphide veins cross-cutting calcite host rock (magnification 4X). Sample DFE3-046-005.**

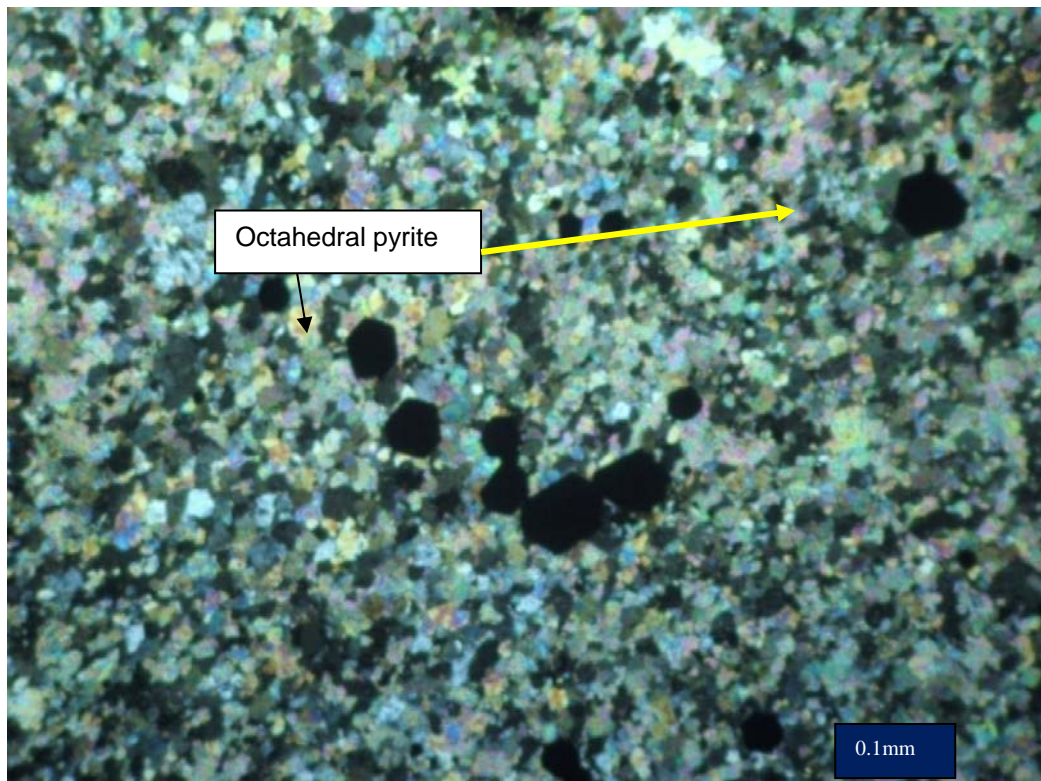


**Fig. 8: Octahedral pyrite in marble (magnification 4X). Sample SDFE3-007-017.**

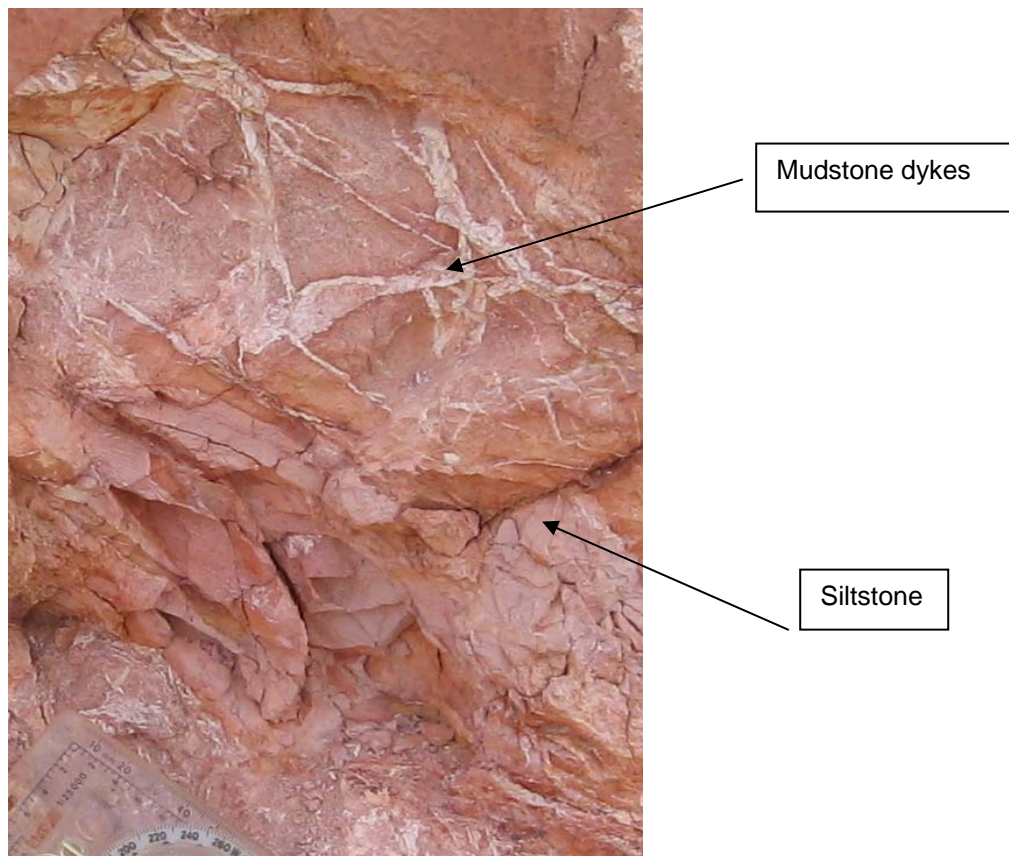


**Fig. 9: Fluid escape structures in the upper slump facies Location: FE3-pit 1; GPS= 1535924; 0215840.**

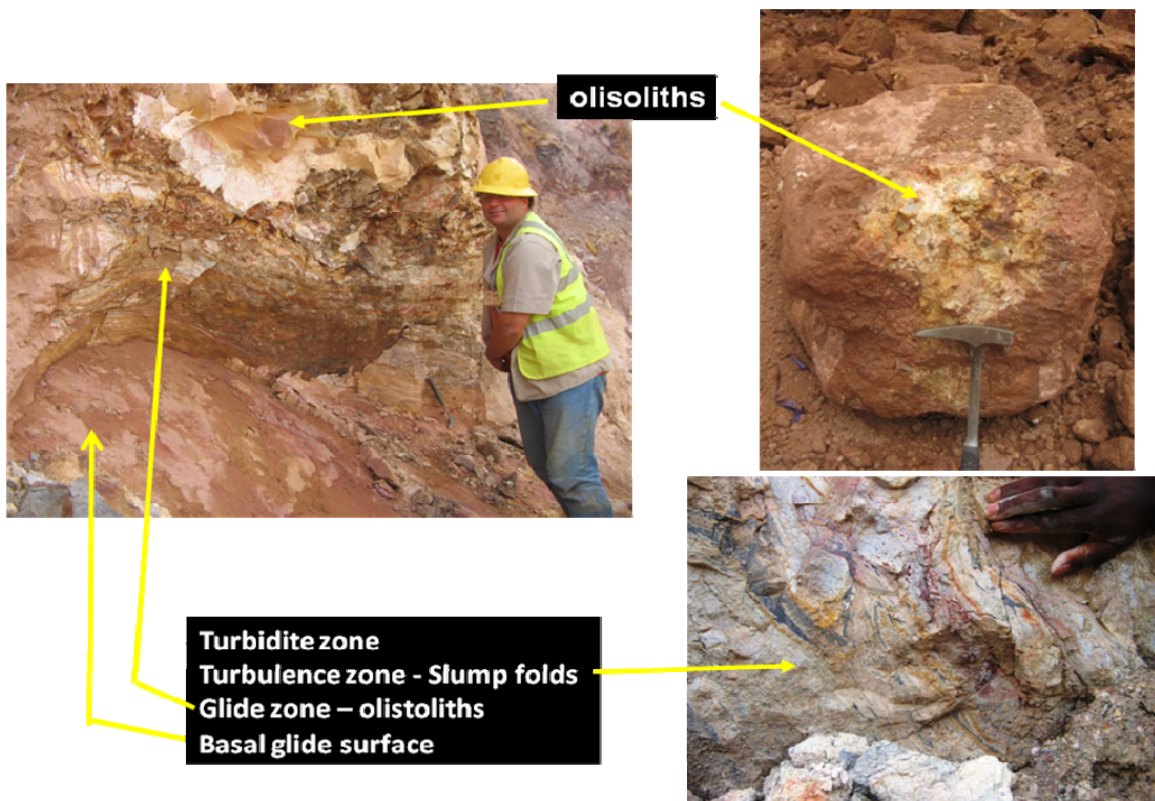


**Fig. 10:** Slumps (with a glide surface, glide zone containing olistoliths and slump folds in the upper slump facies. Location: FE3-pit 2; GPS= 1535190; 0216237.

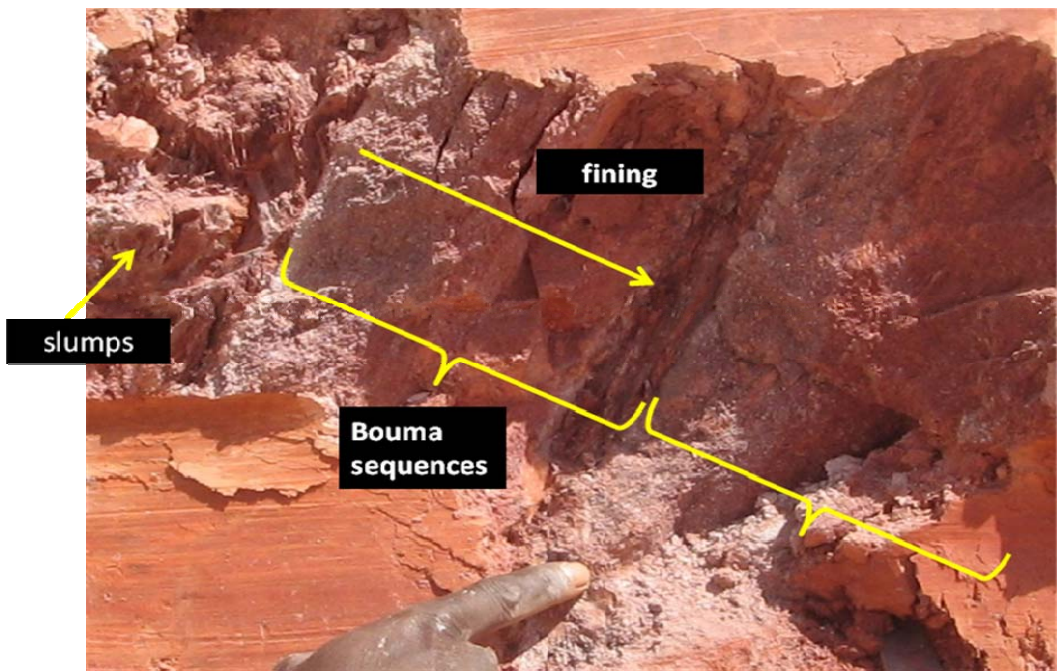


**Fig. 11:** Turbidite beds (with erosion surfaces and fining beds) in the siltstone-greywacke unit.  
 Photo taken from FE4 open cast where the turbidites are overturned and best exposed.



**Fig. 12: Deuteric alteration; (magnification 4X). Sample 195.**

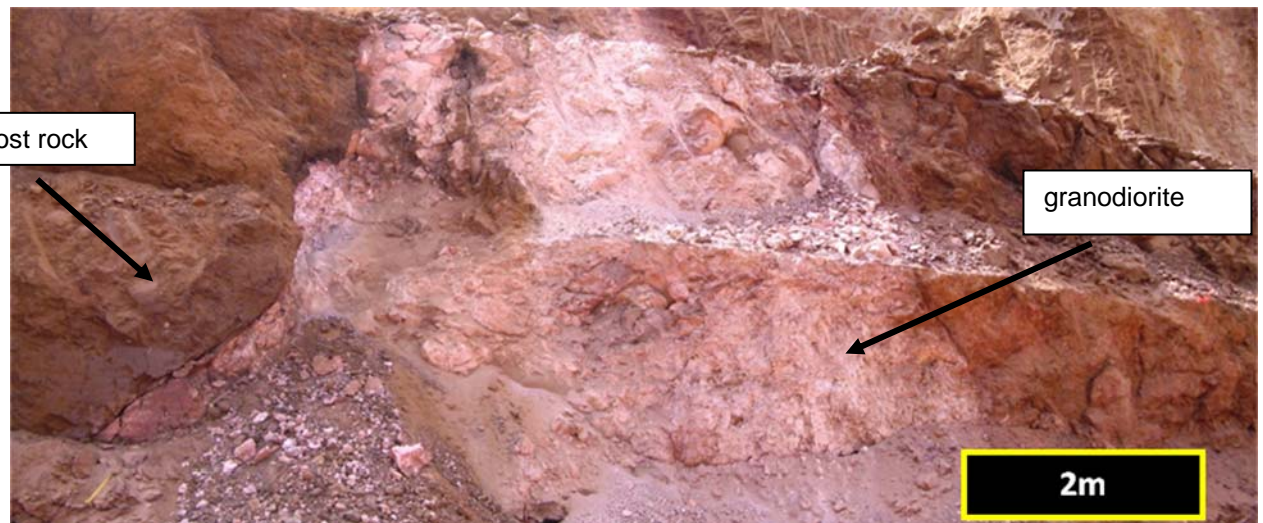


**Fig. 13: Granodiorite dyke; Location: FE3-pit 2; GPS= 1534836; 0216256.**

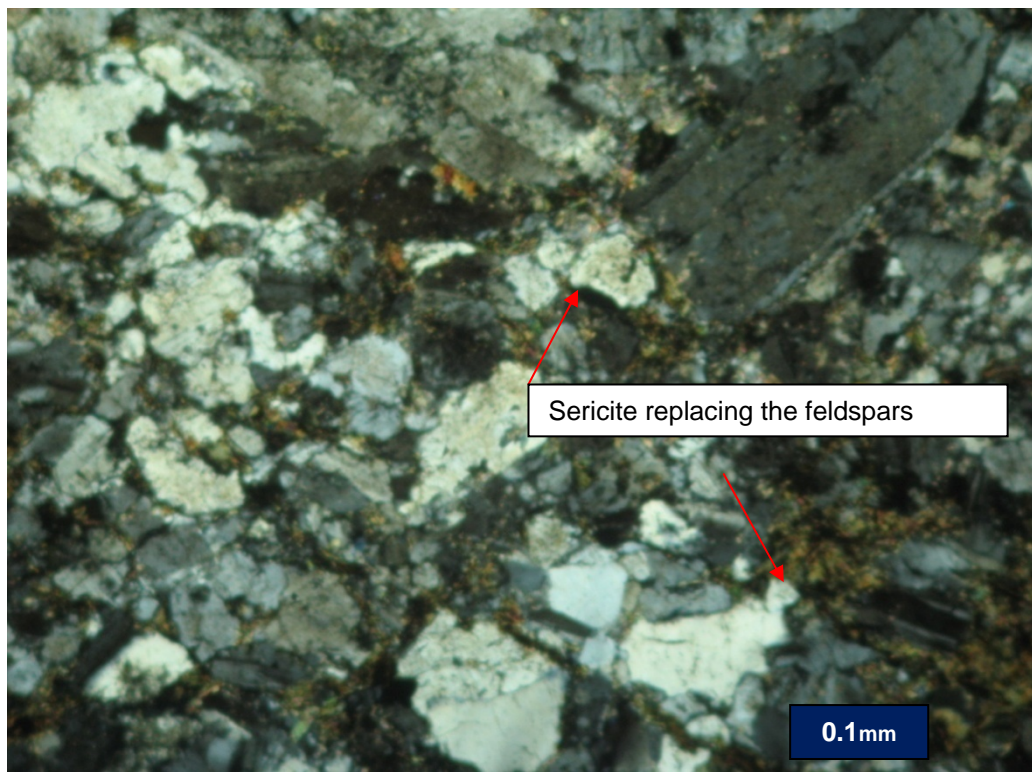
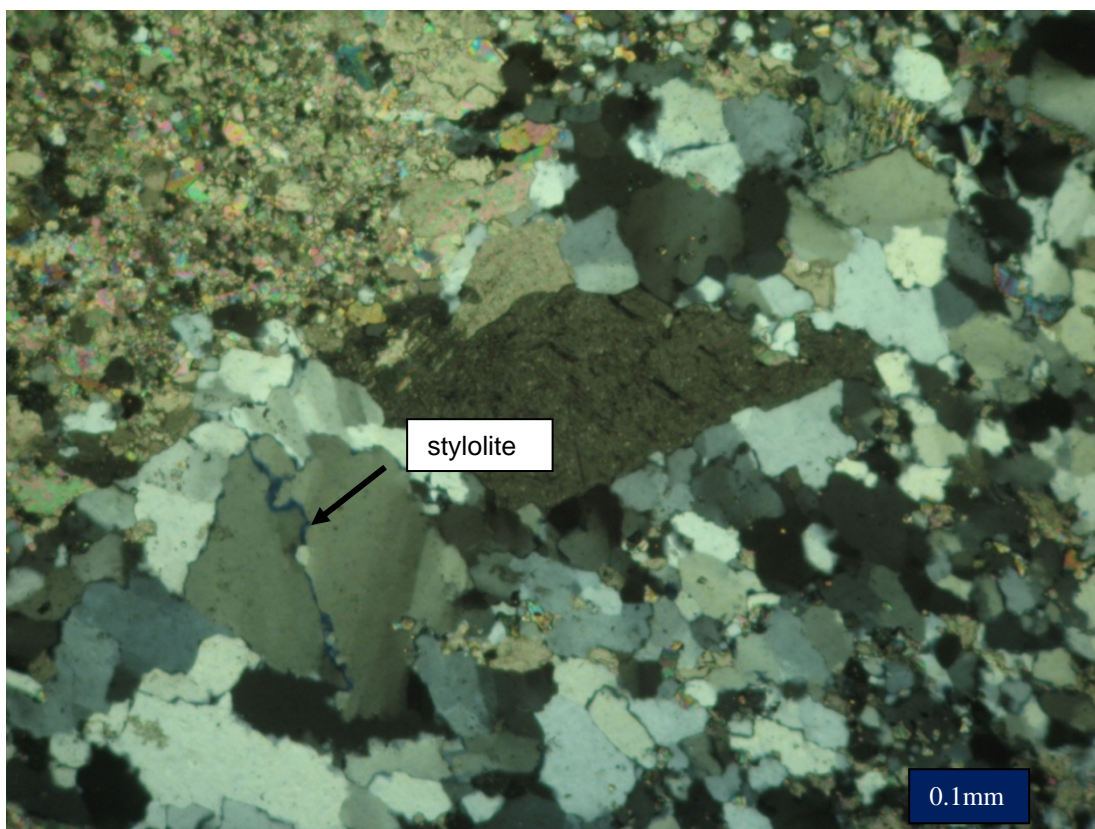


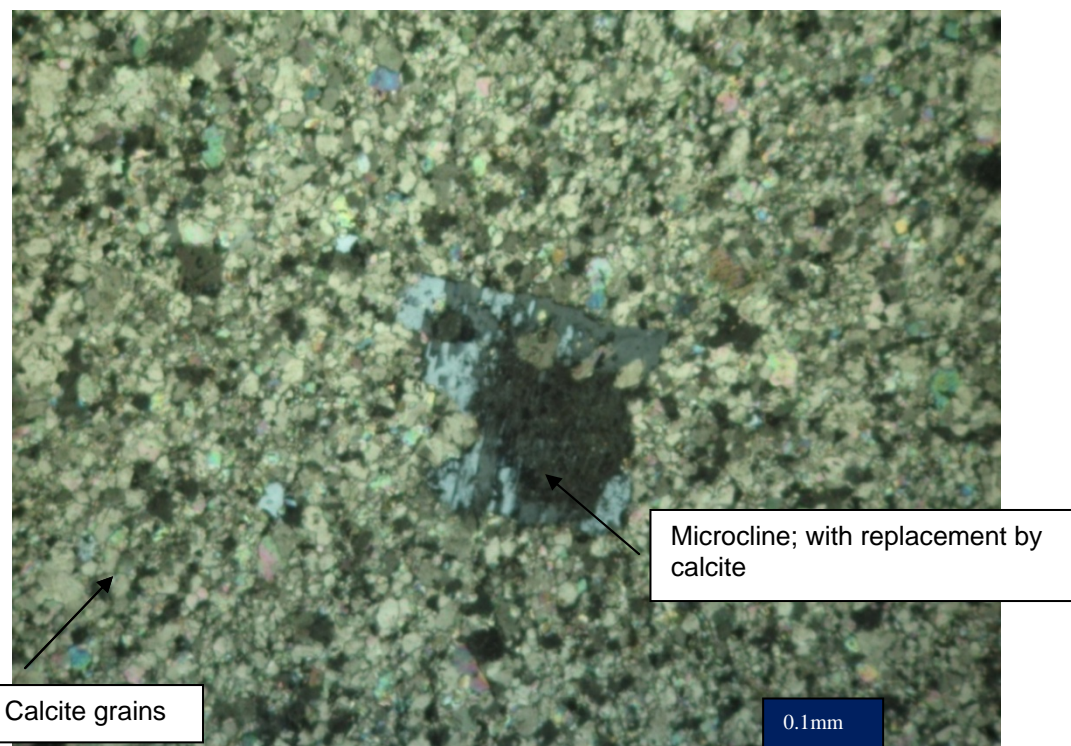
Fig. 14: Sericite alteration in the granodiorite (magnification 4X). Sample 195.



Fig. 15: Breccia consisting of irregular clasts in an iron-oxide matrix. Location: FE3-pit 1;  
GPS= 1535909; 0215872.



**Fig. 16: Granoblastic quartz and micro-stylolites in the greywacke (magnification 4X).**  
**Sample DFE3-046-006.**



**Fig. 17: Microcline in marble with replacement of microcline by calcite (magnification 4X).**  
**Sample SDFE3-007-018.**

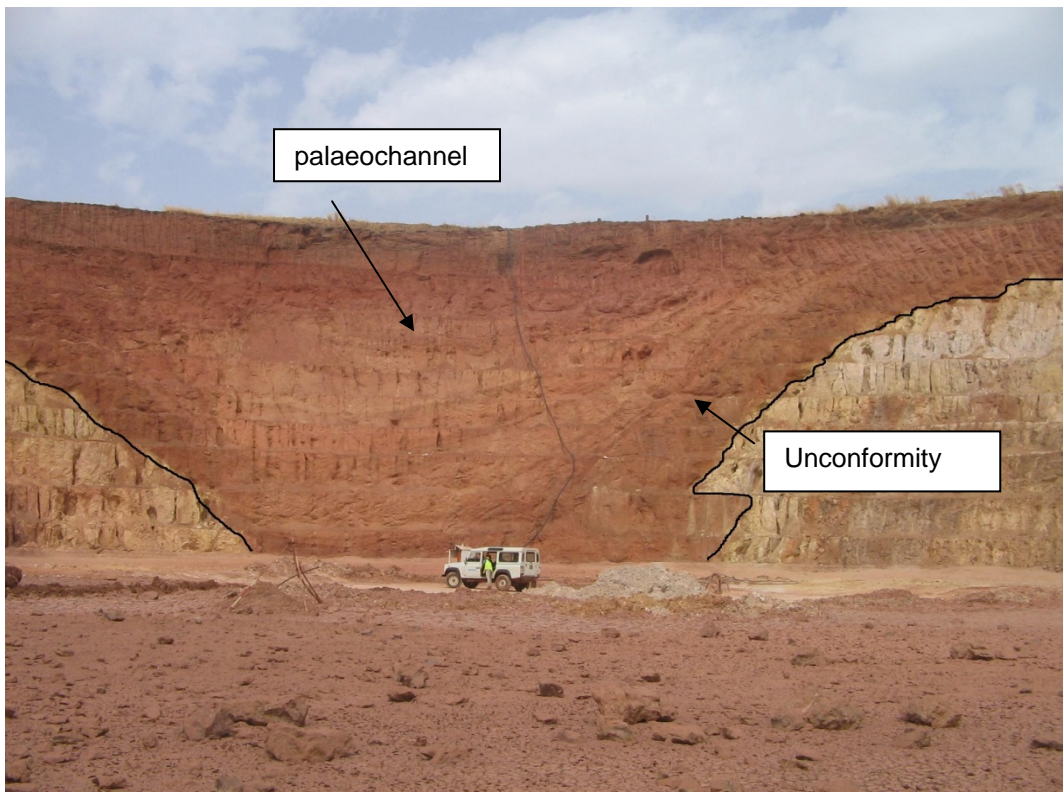


**Fig. 18: Palaeochannel - unconformity at the bottom of the palaeochannel. Location: FE3-pit 3; photo taken facing north.**

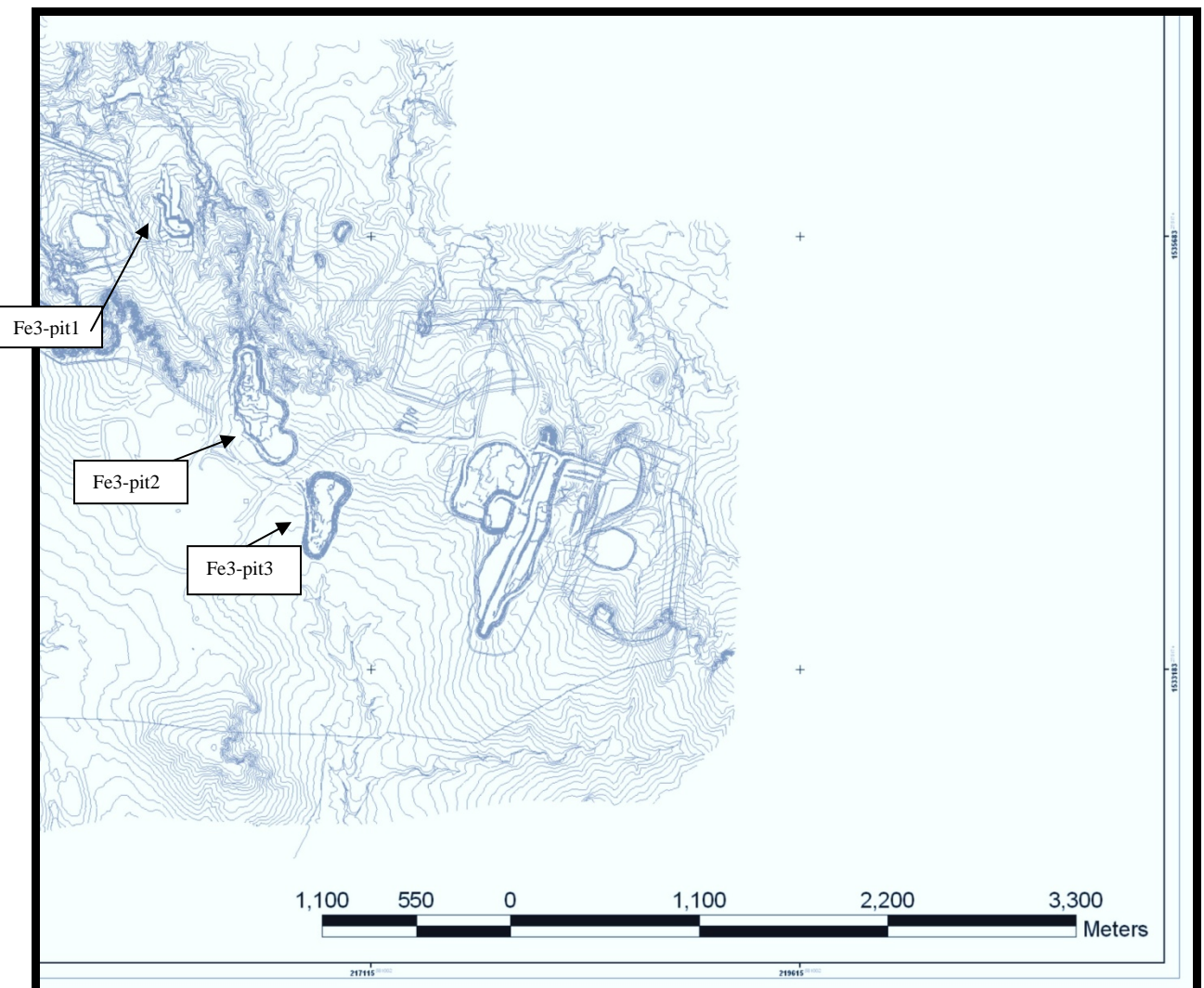
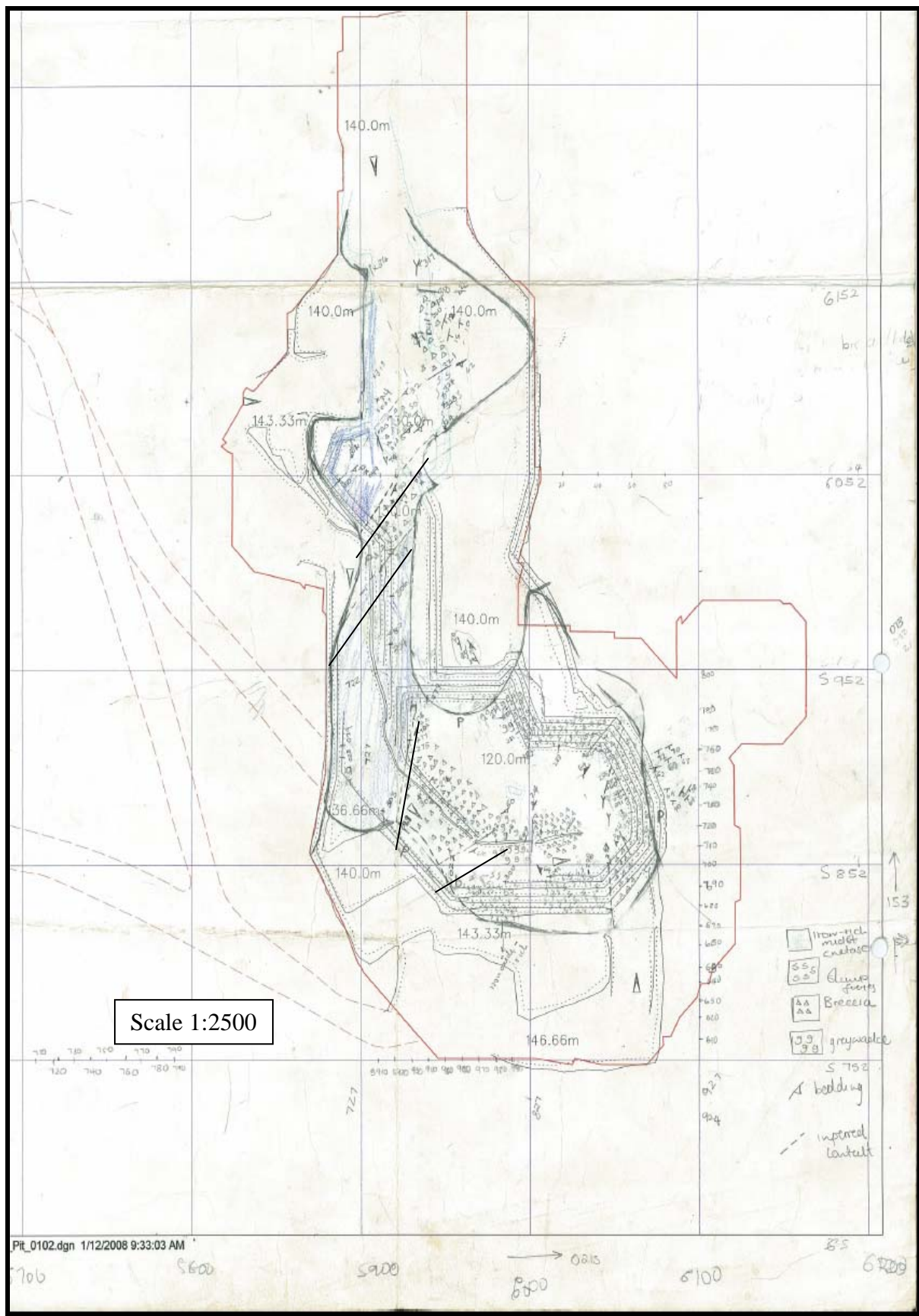
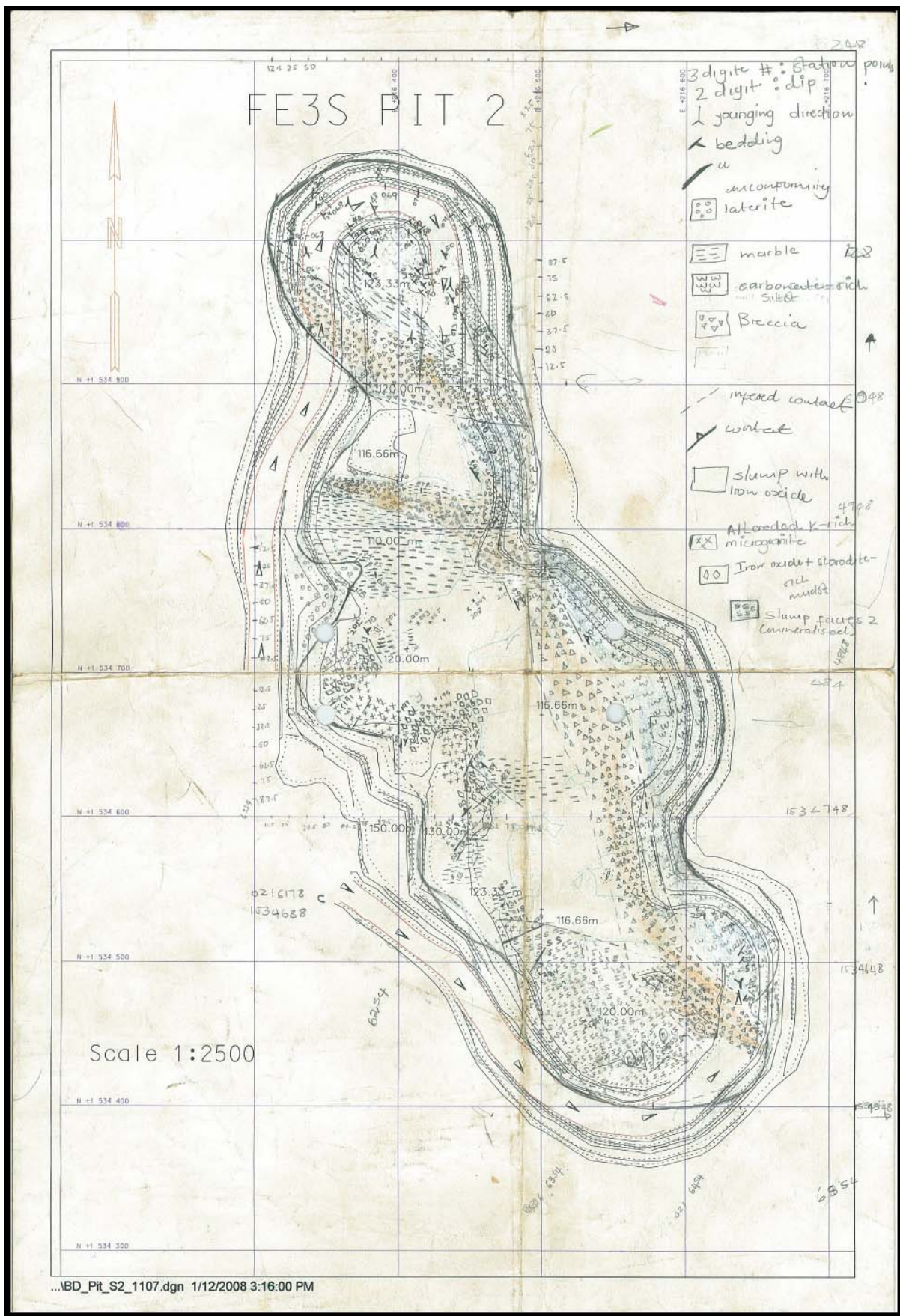


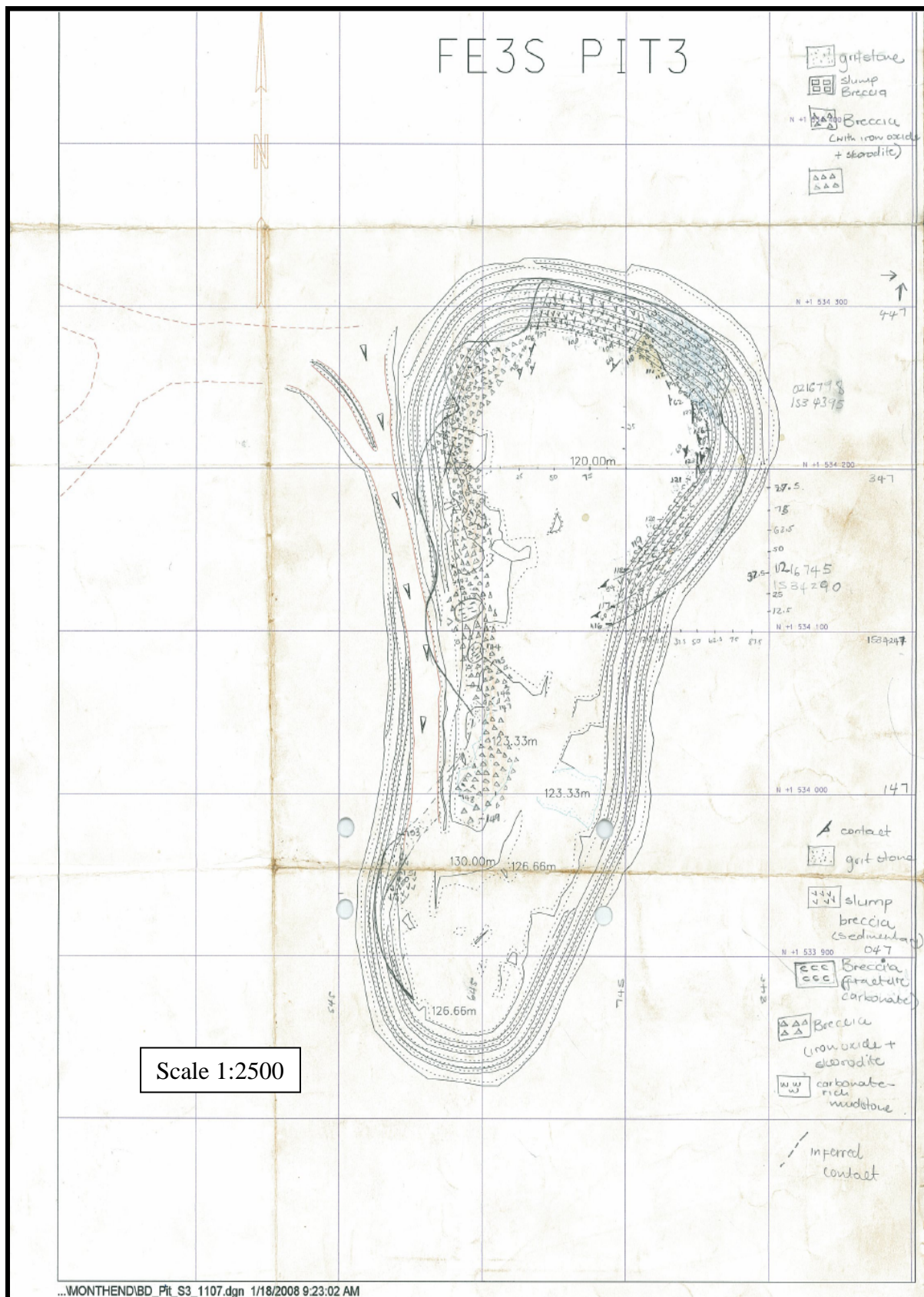
**Fig 19: The Sadiola goldfield.**



### **Map 1: Field map of the FE3 open cast-pit 1.**



**Map 2: Field map of the FE3 open cast-pit 2.**



### **Map 3: Field map of the FE3 open cast-pit 3.**

## **Chapter 5 Discussion**

### **5.1 Depositional Environment**

Slumps characterise the lower and upper slump facies. A slump is a mass-transported debris flow (Martinsen, 1994; Shanmugam, 2000) along the edge of a continental margin. They are a downslope movement of sediment and rock material above a basal shear surface where there is significant internal distortion of the bedding (Stow, 1986). Slump structures form when the sedimentary pile abruptly detaches from a slope and is transported downslope (Collinson et al., 1991). A sediment pile will transport downslope when the shear stress acting within a body of sediment exceeds the shear strength along the slope surface (Dingle, 1980). The sedimentary pile deforms internally (intensely), and produces a variety of deformation structures such as folds, boudins, and micro-faults (Martinsen, 1994), all of which are observed in the study area (Fig. 10).

Ancient slumps have been reported in County Clare, Ireland and in Alexander Island, Antarctica (Farell, 1984; Shanmugam, 2000), and typically along the edge of continental margins. The slumps of County Clare in Ireland represent collapsed slope deposits that were laid down on an unstable basin slope (Collinson et al., 1991). The slumps of Alexandra Island represent mass transported sediments along dislodged from the continental slope into a deep marine environments. Modern slumps are common along continental margins and in modern deltas (The Storegga slumps in Norwegian continental margin; Conway coast in New Zealand; Niger delta continental margin; Mississippi delta-front slumps; slumps in the gulf of Mexico) (Shanmugam et al., 1988; Jansen et al., 1987; Damuth, 1993; McConnico et al., 2007). Slumping can be triggered by gravity, downslope undercutting, and thickening of the sediment pile by deposition, slumping up-slope or seismic activity (Dingle, 1980; Martinsen 1994; Betrand et al., 2008).

From this information slumps of the upper and lower slump facies, which exhibit mass textures, are interpreted to have formed along a continental margin, possible from a stable continental platform

The siltstone-greywacke unit and the upper slump facies are characterised by turbidites beds. Turbidites are deposits of turbidity currents (Meyn et al., 1980; Paciullo et al., 2007). For Newtonian fluids like water, the criterion for the initiation of turbulence is the Reynolds number (Re). The Reynolds number for sediment flow is defined as;

$$Re = P_s \cdot U \cdot h / \mu_s$$

where  $P_s$  = sediment flow density,  $U$  = flow mean velocity,  $h$  = flow thickness and  $\mu_s$  = flow apparent viscosity (Sentini, 1970; Nemec, 1990). For turbulence to be initiated the Reynolds number must be greater than 2000 (Ercilla et al., 2002). High density, fast flowing and deep-water environments are favoured for turbidity currents (Quaeño, 2005). Environments such as these include deep-water and pro-deltaic environments where turbidite sediments readily accumulate (Stow and Johansson 2000; Ponce et al., 2008). From this, it is interpreted that the turbidites in the siltstone-greywacke and the upper slump facies of the FE3 opencasts were deposited in a turbulent environment with deposition in either a pro-deltaic or deep-water environment.

The rootless marble boulders described in Section 4.1.1 are interpreted as olistoliths because the boulders are embedded in slumped siltstone units of the Lower slump facies. An olistostrome (composed of olistoliths) is defined as a sedimentary body of lithological heterogeneous material in which the fine-grained matrix supports the clasts (olistoliths). They can result from sliding and debris flow on the edge of the continental margin (Maltman, 1994; Naylor, 1981). Olistotromes are recorded in Italy and the Niger Delta where slumping and debris flow occur along the passive continental margin (Naylor, 1982; Damuth, 1993). This suggests that the olistostrome were formed along a continental margin where debris flow and mass transportation displaced blocks and rock material downslope.

The mudstone dykes in the upper slump facies are similar to the fluid escape structures described by Lowe (1975), Stromberg, (1998) and Montenat et al. (2007) who interpreted mudstone and carbonate dykes as injection dykes (Fig. 20). Injection dykes are a class of seismite developed by soft sediment deformation processes (Mazumder et al., 2006; Montenat et al., 2007). They are caused by seismic shocks commonly induced by earthquakes and form as a result of hydrofracturing and fluidisation. (Fuller, 1912 in Montenat et al., 2007). A fracture network is formed in relatively cohesive sediment during a seismic event and soft sediments, such as mud, percolate into the fracture network (Montenat et al., 2007; Foix et al., 2008). It is possible that the mudstone dykes in the upper slump facies of the FE3 opencasts formed seismically active environment.

Shanmugam (1997) also proposed a non-seismic model for the formation of fluid escape structures. The fluid escape structures are a feature of rapid sedimentation (Shanmugam, 1997; 2000) and gravity induced sliding (Collinson et al, 1991). When sediments are deposited at a relatively fast rate, fluid is trapped within the sediments, such that the sediments are suspended in fluid (Foix et al., 2008). The grains settle into a grain framework

and as a result the fluid trapped in the sediments is squeezed through the pore space network (Lowe, 1975). Fluid escapes by percolating upwards through the sediments and the vein network represents the pathways along which the fluid movement occurred (Lowe, 1975). Therefore, it may also be possible that the fluid escape structures formed in a gravity-induced slump environment.

The contact between the upper slump facies and the greywacke unit represents a change in depositional environment. Because of limited outcrop exposure and deep weathering it is not well exposed but must represent an unconformity (*sensu stricto*). In the nearby Sadiola opencast (6 kms west) the greywacke unit is massive, laminated and crossbedded (Hein et al., 2008), with no evidence of slump or debris flows. It is interpreted to have been deposited in a shallow marine tidal environment. The greywacke unit at the FE3 opencast thus represents a change in depositional environment towards shallow marine tidal. The unconformity therefore represents a drop in sea level or regression along the delta, or uplift.

In summary, slumps in the upper and lower slump facies indicate that there was mass transportation, slumping and debris flow along a (possible) continental margin during deposition. Turbidites units in the upper slump facies and siltstone-greywacke unit were deposited in turbulent environment, possibly in pro-deltaic or deep-water environment. The mudstone dykes of the upper slump facies are interpreted to represent a class of seismites called sedimentary injection dykes which are formed in a seismically active environment or under gravity-induced collapse. Seismic activity or gravity-induced collapse is interpreted as the triggering mechanism for mass transport and debris flow. The greywacke unit unconformably overlying the siltstone-greywacke is interpreted to represent a significant change in depositional environment following the deposition of the siltstone-greywacke unit.

Further to this, the marble boulders embedded in the lower slump facies host cube-pyritohedrons with relict pyrrhotite (Fig. 8). Experimental studies on the morphology of pyrites by Graham and Ohmoto (1994) demonstrated that the growth of octahedral pyrite (on pyrrhotite surfaces) requires the presence of excess CaSO<sub>4</sub> (gypsum) leading to the possibility that CaSO<sub>4</sub> (gypsum) was found in excess in the provenance environment of the boulders. If correct the source region for the marble may have been an evaporative shallow marine environment (Schröder et al., 2006). Also marble is a metamorphic rock and the pyritohedrons are the product of recrystallization. This indicates the provenance area of marble was subjected to metamorphism.

The deposition of carbonate occurs in a relative stable depositional environment (Poyer et al., 2008). Slope and shallow marine carbonate can be re-sedimented into a slump environment by the processes of debris fall and sliding as olistoliths (Naylor, 1982; Martinsen, 1994). Debris fall and flow are common processes along the pro-delta (Manzi et al., 2007; Pierre et al., 2006; Dennielou et al., 2006). Debris flow of a carbonate platform requires a triggering mechanism that destabilizes the environment to form olistostrome. Debris flow can be triggered by gravity, active earthquakes or seismic shocks (Montenat et al., 2007; McConnico et al., 2007; Damuth, 1993). In this case, the marble olistoliths in the FE3 opencasts were re-sedimented into a slump environment by debris flow and slumping along a continental margin.

Finally, the sediments of the FE3 opencasts (Kofi Series) have not been dated but are interpreted as Birimian in age by Hirdes et al. (2002). The Birimian sequences of the West African craton are dated at 2238-2171 Ma (Milési et al., 1991, 1992; Ledru et al., 1991; Boher et al., 1992). The Birimian sequences are composed of tholeiitic basalts, andesitic volcanic, calc-alkaline volcanics, volcaniclastic sediments, detrital sediments and chemical sediments which are characteristic of an oceanic island arc environment (Hirdes et al., 2002; Gueye et al., 2008). In contrast, the Birimian sequences of the Kéniéba Inlier (i.e., Mako Supergroup; Diale-Daleme Supergroup; Falemé volcanic belt) are dated at  $2063 \pm 41$  Ma,  $2096 \pm 8$  Ma +  $2099 \pm 4$  Ma (respectively). They are interpreted as remnants of an oceanic island arcs terrane that was accreted onto an Archaean continent (Diallo, 2001; Dia et al., 1997). There is a considerable difference between the ages given for the Birimian sequences of the West African craton and those of the Kénieba Inlier as indicated in Fig 22 and accord better, but are still younger, than those of the Tarkwa Group (2149-2132 Ma; U-Pb zircon, Davis et al., 1994) which unconformably overlies the Birimian. It is therefore suggested that the slump, olistostrome, turbidite, siltstone-greywacke and greywacke sediments of the FE3 opencasts were derived from the erosion of the Birimian terrane.

## **5.2 Gold bearing breccias and veins**

The structures that host mineralisation in the region are breccia and quartz-arsenopyrite veins that crosscut the stratigraphy, which implies that gold mineralisation is younger than the sedimentary units. The mineralised breccias (and associated alteration, Fig. 21) occur around contact aureole of the granodiorite. This may imply that the mineralisation is related to the intrusion of the granodiorite as has been established in the nearby Sadiola deposit by Hein and Tshibubudze (2007b). The granodiorite dykes show evidence of fluid circulation as represented by deuterian alteration and sericitisation. Similar deuterian alteration and sericitisation textures have been reported by Candela (1994) and Yuguchi et al. (2007) and

may be the result of dissolution and re-precipitation related to fluid movement. This suggest that there was fluid circulation associated with the granodiorite however is not clear whether the fluids are contact metamorphic or magmatic.

The Kéniéba Inlier was intruded by granitoids during the Eburnean Orogeny. Two major magmatic events have been identified in the Inlier; at 2.16-2.11 Ga and at 2.08-2.07 Ga (Gueye et al., 2008).

### **5.3 Secondary placer gold mineralisation**

Placer gold mineralisation is hosted at the base of the palaeochannels. These palaeochannel crosscut the mineralised breccias and the lower slump facies. This suggests that the palaeochannels are younger than the primary mineralised zones. The source of the gold is interpreted to be derived from the erosion the primary hydrothermal gold mineralisation.

### **5.4 Geological history**

The geological history of the FE3 open cast: -

1. Deposition of the lower slump facies.
2. Deposition of the upper slump facies
3. Deposition of the siltstone-greywacke unit.
4. Erosion followed by the deposition of the greywacke unit during marine regression or uplift.
5. Development of a weak shear localised in the Siltstone-Greywacke unit.
6. Intrusion of the granodiorite dykes and the Sekokoto pluton. The intrusion was accompanied by contact metamorphism around the intrusive rocks. Also the intrusion resulted in the circulation of magmatic-hydrothermal fluids in the sedimentary sequences and in the dykes. Gold-bearing breccias possibly formed at this time.
7. Erosion and the development of the palaeochannels and deposition of the placer gold mineralisation.
8. Erosion and development of the laterite profile.

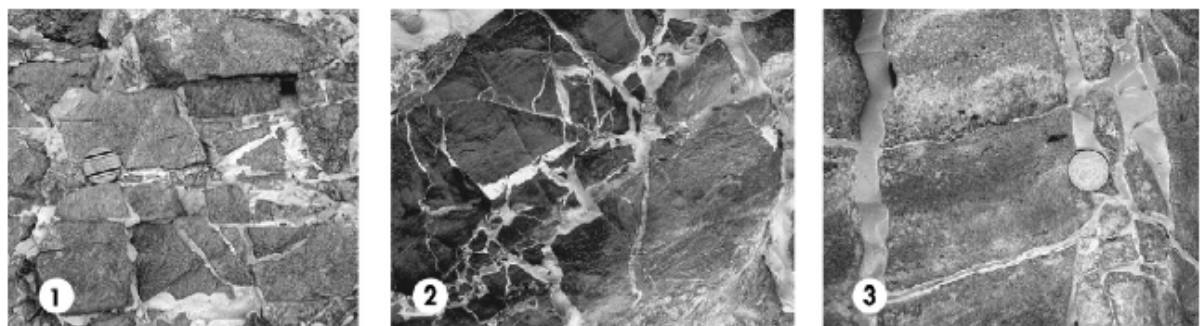


**Fig. 20: Injection dykes from Messina Strait and Capo Millazo (modified from Montenat et al., 2007).**

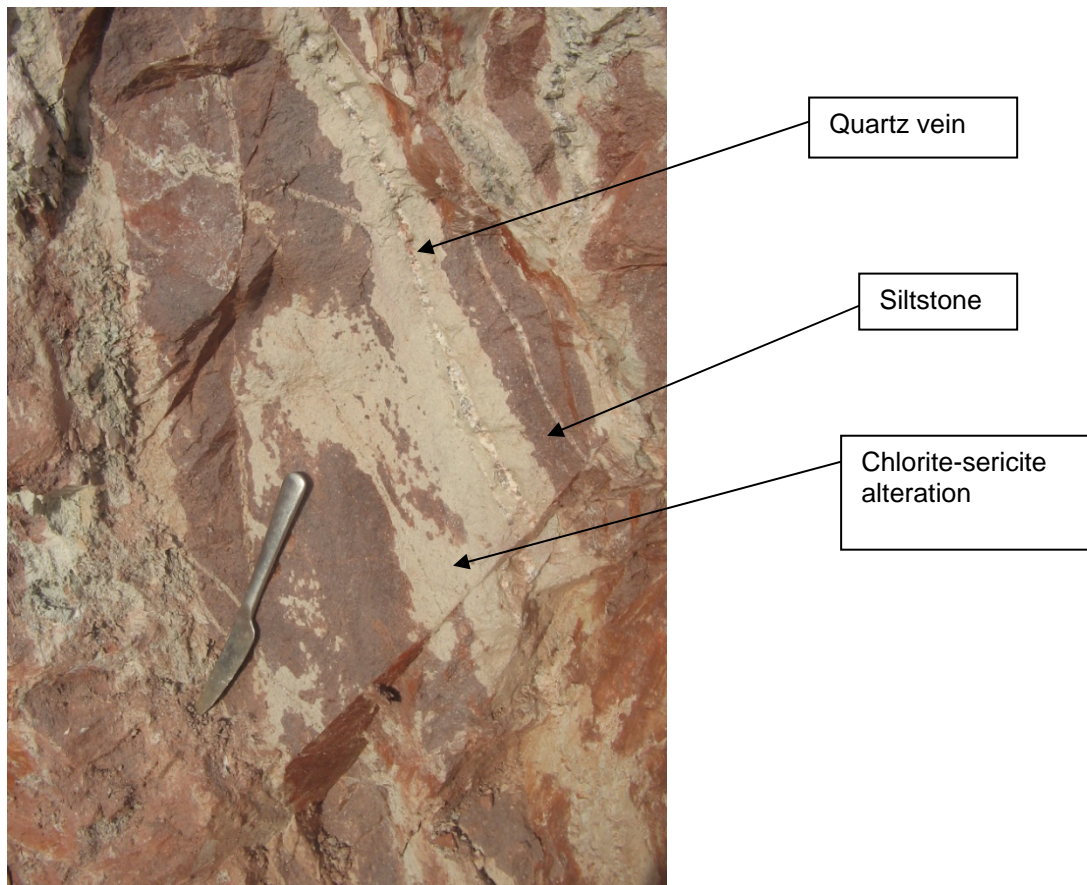


**Fig 21: Sericite and chlorite alteration in siltstones around quartz veins.**

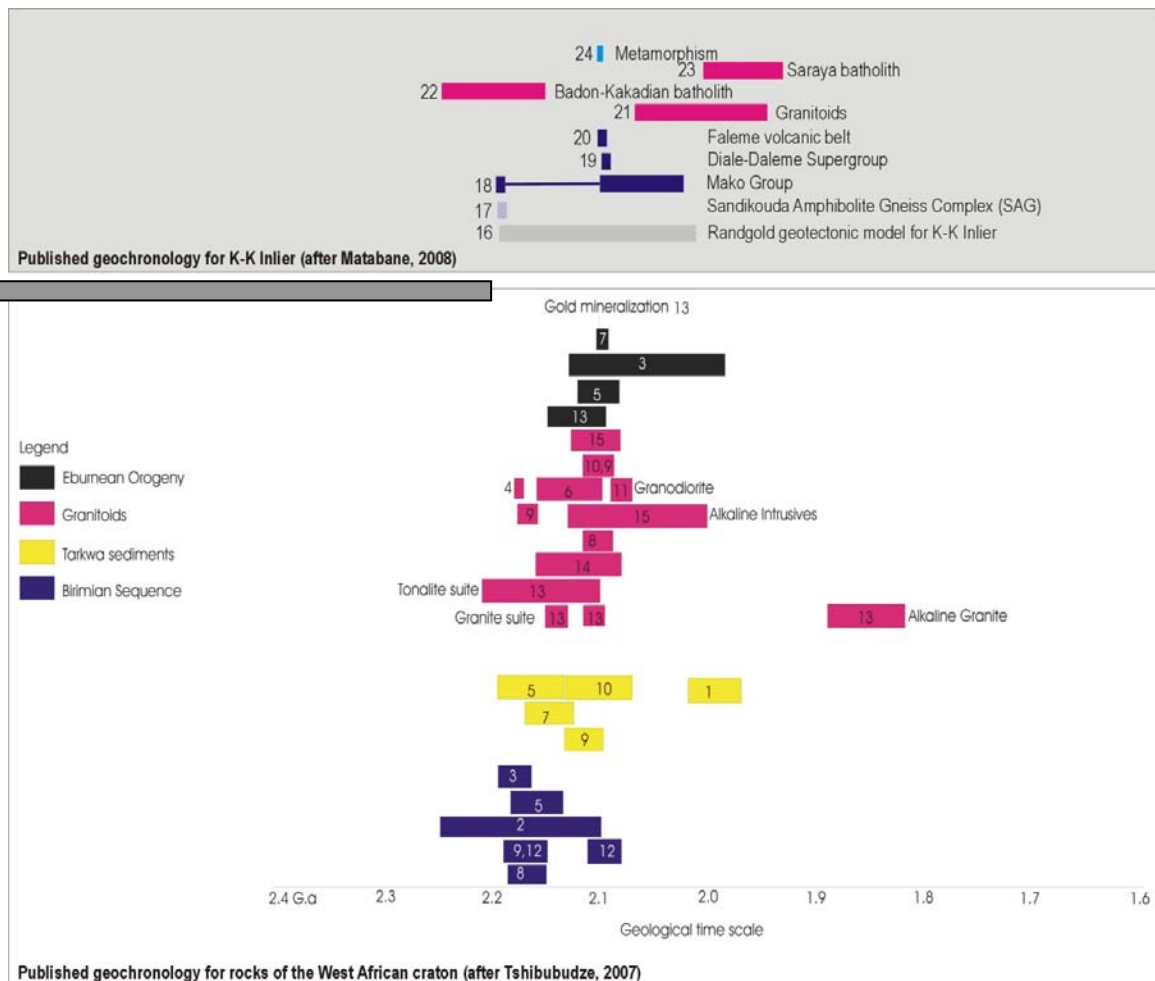


**Fig. 19 (with permission from Hein et al., 2008)**

**Published absolute geochronology for rocks of the West African Craton:**

**1, 4, 8,** Hirdes et al. (1987, 1992, 1996); **2,** Milési et al. (1989); **3,** Leube et al. (1990); **5,** Davis et al. (1994); **6,** Pons et al. (1995); **7,** Bossière et al. (1996); **9, 12,** Hirdes and Davis (1998, 2002); **10,** Oberthür et al. (1998); **11,** Egal et al. (2002); **13,** Castaing et al. (2003); **14,** Dioh et al. (2006); **15,** Feybesse et al. (2006).

**Published absolute geochronology for KK- Inlier:**

**16.** Holliday (2008); **17.** Dia et al. (1997, Pb-Pb age), Pawlig et al. (2006,  $T_{DM}$  Sm-Nd ); **18.** Dia et al. (1997; Detrital zircons, Pb-Pb age), Abouchami (1990, Sm-Nd); **19.** Ledru et al. (1991; Pb-zircon evaporation), Hirdes et al. (2002); **20.** Hirdes et al. (2002, Pb-Pb age); **21.** Ledru et al. (1991); Taylor et al. (1992, Pb-Pb); Pali et al. (2006). **22.** Bassot and Caen-Vachette (1984 in Ledru et al., 1991, Rb-Sr whole rock); Gueye et al. (2008); **23.** Ledru et al. (1991; Rb-Sr); **24.** Hirdes et al (2002); Pawlig et al. (2006, U-Pb age on sphene).

## **6. Conclusions**

1. The lithologies of the FE3 opencasts (FE3\_1, FE3\_2 and FE3\_3) can be divided into four major units; lower slump facies, an upper slump facies, a siltstone-greywacke and a greywacke unit.
2. Slumps of the upper and lower slump facies, which exhibit mass flow textures (glide surfaces, slump folds, chaotic bedding, floating clast, olistoliths, turbidites, seismites and fluid escape structures) are interpreted to have formed along a continental margin in either a pro-deltaic or deep-water environment, possible from a stable continental platform.
3. Olistoliths (marble, mudstone, etc) embedded in slumped siltstone units of the Lower Slump facies are were the result of mass transport of carbonate blocks and rock material downslope from a stable carbonate platform. Pyritohedrons in marble olistoliths may indicate an evaporative shallow marine environment.
4. Mudstone dykes are common in the upper slump facies. The dykes were possibly produced by seismic activity or gravity-induced collapse.
5. A siltstone-greywacke sequence overlies the upper slump facies is crossbedded.
6. The contact between the upper slump facies and the greywacke unit represents a change in depositional environment marked by a drop in sea level or regression along the delta, or uplift.
7. The above stratigraphy has been intruded by granodiorite dykes that are deuterically altered and sericitised.
8. There are two phases of mineralisation in the study area. (a) Primary hydrothermal mineralisation: Gold mineralisation in the breccia lodes and in the upper slump facies consists of arsenopyrite-pyrite-gold assemblages; (b) Secondary placer gold mineralisation.
9. A laterite profile covers the study area to a thickness of more than 2 metres
10. The considerable difference between the ages given for the Birimian sequences of the West African craton and those of the Kenieba Inlier could indicate that the slump, olistostrome, turbidite, siltstone-greywacke and greywacke sediments of the FE3 opencasts were derived from the erosion of the Birimian terrane.

## **References**

- Abouchami, W., Bohr, M., Michard, A., Albarede, F., 1990. A major 2.1 Ga event of mafic magmatism in West Africa: an early stage of crustal accretion. *Journal of Geophysical Research* 95 (B11), 17605-17629.
- Bassot, J.P., Caen-Vachette, M., 1984. Données géochronologiques et géochimiques nouvelles sur les granitoïdes de l'Est Sénégal: implications sur l'histoire géologique du Birrimien de cette région. In: J. Klerkx and J. Michot (Editors), *Géologie Africaine*. Musée royal, Tervuren, pp. 191-1106.
- Bassot, J.P., Doimangdt, A., (1986). Mise en évidence d'un accident majeur affectant le Protérozoïque inférieur des confins sénégalo-maliens. *Comptes Rendus Académie Sciences Paris* 302, 1101-1106.
- Bertrand, S., Charlet, F., Chapron, E., Fagel, N., De Batist M., 2008. Reconstruction of the Holocene seismotectonic activity of the Southern Andes from seismites recorded in Lago Icalma, Chile, 39°S. *Palaeogeography, Palaeoclimatology, Palaeoecology* 259, 301-322.
- Béziat, D., Dubois, M., Debat, P., Nikiéma, S., Salvi, S., Tollen, F., 2008. Gold metallogeny in the Birimian craton of Burkina Faso (West Africa). *Journal Africa Earth Science* 50, 215-233.
- Boher, M., Abouchami, W., Michard, A., Albarede, F., Arndt, N.T., 1992. Crustal growth in West Africa at 2.1 Ga. *Journal of Geophysical Research* 97 (B1), 345-369.
- Bossière, G., Bonkoungou, I., Peucat, J.J., Pupin, J.P., 1996. Origin and age of Palaeoproterozoic conglomerates and sandstones of the Tarkwaian Group in Burkina Faso, West Africa. *Precambrian Research* 80, 153-172.
- Brown, E.T., Bourlés, D.L., Colin, F., Sanfo, Z., Raisbeck, G.M., Yiou, F., 1994. The development of iron crust lateritic systems in Burkina Faso, West Africa examined with in-situ-produced cosmogenic nuclides. *Earth and Planetary Science Letters* 124, 19-33.
- Candela, P.A., 1994. Combined chemical and physical model for plutonic devolatilization: A non-Rayleigh fractionation algorithm. *Geochimica et Cosmochimica Acta* 58, 2157-2167.
- Collinson, J.D., Martinsen, O.J., Bakken, B., Kloster, A., 1991. Post-glacial mass flow and associated deposits preserved in palaeovalleys: a complex relationship between turbidites and deltas. *Basin Research* 3, 223-242.
- Damuth, J.E., 1993. Neogene gravity and depositional processes on the deep Niger delta continental margin. *Marine and Petroleum Geology* 11, 320-327.

- Davis, D.W., Hirdes, W., Schaltegger, U., Nunoo, E.A., 1994. U-Pb age constraints on deposition and provenance of Birimian and gold-bearing Tarkwaian sediments in Ghana, West Africa. *Precambrian Research* 67, 89-107.
- Debat, P., Nikiéma, S., Mercier A., Lombo, M., Béziat D., Bourges, F., Roddaz, M., Salvi, S., Tollon, F., Wenmenga, U., 2003. A new metamorphic constraint for the Eburnean orogeny from Palaeoproterozoic formations of the Man shield (Aribinda and Tampelga countries, Burkina Faso). *Precambrian Research* 123, 47-65.
- Dennielou, B., Huchon, A., Beaudouin C., Berné, S., 2006. Vertical grain-size variability within a turbidite levee: Autocyclicity or allocyclicity? A case study from the Rhône neofan, Gulf of Lions, western Mediterranean. *Marine Geology* 234, 191-213.
- Dia, A., Van Schmus, W. R., Kröner,, A., 1997. Isotopic constraints on the age and formation of a Palaeoproterozoic volcanic arc complex in the Kedougou Inlier; eastern Senegal, West Africa. *Journal of African Earth Sciences* 24, 197-213.
- Diallo, D.P., 2001. Le paléovolcanisme de la bordure occidentale de la boutinnière de Kédougou, Paléoprotérozoïque du Sénégal oriental: incidences géotectoniques. *Journal of Earth Sciences* 32, 919-940.
- Dingle, R.V., 1980. Large allochthonous sediment masses and their role in the construction of the continental slope and rise off southwestern Africa. *Marine Geology* 37, 333-354.
- Dioh, E., Béziat, D., Debat, P., Grégoire, M., Ngom, P.M., 2006. Diversity of the Paleoproterozoic granitoids of the Kedougou inlier (eastern Senegal): Petrographical and geochemical constraints. *Journal of African Earth Sciences* 44, 351-371.
- Komla, D-A., 1993. Geology and geochemical patterns of the Birimian geological deposits, Ghana, West Africa. *Journal of Geochemical Exploration* 47, 305-320.
- Egal, E., Thiéblemont, D., Lahondére, D., Guerrot, C., Costea, C.A., Iliescu, D., Delor, C., Goujou, J.C., Lafon, J.M., Tegyey, M., Diaby, S., Kolié, P., 2002. Late Eburnean granitization and tectonics along western and northwestern margin of the Archaean Kenema-Man domain (Guinea, West African craton). *Precambrian Research* 117, 57-84.
- Eisenlohr, B.N., Hirdes, W., 1991. The structural development of the early Proterozoic Birimian and Tarkwaian rocks of southwest Ghana, West Africa. *Journal of African Earth Sciences* 14, 313-325.
- Ercilla, G., Alonso, B., Wynn, R.B., Baraza, J., 2002. Turbidity current sediment waves on irregular slopes observation from the Orinoco sediment-wave field. *Marine Geology* 192, 171-187.
- Farrell, S.G., 1984. A dislocation model applied to slump structures. *Journal of Structural Geology* 6, 727-736.

- Feybesse, J., Billa, M., Guerrot, C., Duguey, E., Lescuyer, J., Milési, J., Bouchot, V., 2006. The Palaeoproterozoic Ghanaian Province: Geodynamic model and ore controls, including regional stress modelling. *Precambrian Research* 149, 149-196.
- Foix, N., Paredes, J.M., Giacosa, R.E., 2008. Paleo-earthquakes in passive-margin settings, an example from the Paleocene of the Golfo San Jorge Basin, Argentina. *Sedimentary Geology* 205, 67-78.
- Fouillac, A.M., Dommangeat, A., Milési, J.P. 1993. A carbon, oxygen, hydrogen and sulfur isotopic study of the gold mineralization at Loulo, Mali. *Chemical Geology* 106, 47-62.
- Graham, U.M., Ohmoto, H., 1993. Experimental study of formation mechanisms of hydrothermal pyrite. *Geochimica et Cosmochimica Acta* 58, 2187-2202.
- Gueye, M., Ngom, P.M., Diène, M., Thiam, Y., Siegesmund, S., Wemmer, K., Pawlig, S., 2008. Intrusive rocks and tectono-metamorphic evolution of the Mako Palaeoproterozoic belt (Eastern Senegal, West Africa). *Journal of African Earth Sciences* 50, 88-110.
- Hein, K.A.A., 2003. Relative timing of deformational, metamorphic and mineralisation events at the Mt. Todd (Yimuyn Manjerr) Mine, Pine Creek Inlier, Northern Territory, Australia. *Ore Geology Reviews* 22, 143–175.
- Hein, K.A.A., Tshibubudze, A., 2007a. Sadiola Ore Genesis Model, Sadiola Mine and satellite pits, Mali. Final company report to Societe D'Exploitation des Mines d'Or de Sadiola S.A. (SEMOD), Mali, August 2007, 15p
- Hein, K.A.A., Tshibubudze, A. 2007b. Sadiola Ore Genesis Model, Sadiola Mine and satellite pits, Mali. Report to Société d'Exploration des Mines d'Or de Sadiola S.A., Mali., 8p.
- Hein, K.A.A., Tshibubudze, A., Matabane, M.R., 2008. Geology and gold metallogenesis of the Sadiola goldfield, Mali. Report to Société d'Exploration des Mines d'Or de Sadiola S.A., Mali., 38p.
- Hirdes, W., Davis, D.W., 2002. U-Pb Geochronology of Palaeoproterozoic rocks in the southern part of the Kedougou-Kéniéba Inlier; Senegal, West Africa: Evidence for Diachronous Accretionary Development of the Eburnean Province. *Precambrian Research* 118, 83-99.
- Hirdes, W., Davis, D.W., Eisenlohr, B.N., 1992. Reassessment of Proterozoic granitoid ages in Ghana on basis of U/Pb zircon and monazite dating. *Precambrian Research* 56, 89-96.
- Hirdes, W., Davis, D.W., Lüdtke, G., Konan, G., 1996. Two generations of Birimian (Paleoproterozoic) volcanic belts in north-eastern Côte d'Ivoire (West Africa): consequences for the 'Birimian Controversy'. *Precambrian Research* 80, 173-191.

- Holliday, J., 2008. The Kedougou-Kenieba Inlier: An emerging world-class gold district. Randgold Resources. Africa Uncovered conference. Misty Hills, Johannesburg. 05 July 2008.
- Jansen, E., Benfring, S., Bugge, T., 1987. Large submarine slides on the Norwegian continental margin: sediments, transport and timing. *Marine Geology* 78, 77-107.
- Ledru, P., Milési, J.P., Vinchon, C., Ankrah, P.T., Johan, V., Marcoux, E., 1988. Geology of the Birimian series of Ghana. In: Abstract of international Conference and workshops on the geology of Ghana with special emphasis on Gold, geology and exploration in Ghana and selected other Precambrian terrains, 75<sup>th</sup> anniversary, Ghana Geological Survey Dept. Accra Ghana, pp. 26-27.
- Ledru, P., Pons, J., Milési, J.P., Feybesse, J.L., Johan, V., 1991. Transcurrent tectonics and polycyclic evolution in Lower Proterozoic of Senegal-Mali. *Precambrian Research* 50, 337-354.
- Lemoine, S., Tempier, P., Bassot, J. P., Caen-Vachette, M., Vialette, Y., Touré, S., Wenmenga, U., 1990. The Burkinian orogenic cycle; precursor of the Eburnian orogeny in West Africa. *Geology Journal* 25, 171- 188.
- Leube, A., Hirdes, W., Mauer, R., Kesse, G., 1990. The Early Proterozoic Birimian Supergroup of Ghana and Some aspects of its Gold Mineralisation. *Precambrian Research* 46, 139-165.
- Liégeois, J.P., Claessens, W., Camara, D., Klerkx, J., 1991. Short lived Eburnean orogeny in southern Mali. *Geology, tectonics, U-Pb and Rb-Sr geochronology*. *Precambrian Research* 50, 111-136.
- Lowe, D.R., 1975. Water escape structures in coarse-grained sediments. *Sedimentology* 22, 157-204.
- Maltman, A., 1994. Introduction and overview. In: *The geological deformation of sediments* (1<sup>st</sup> edition). Chapman and Hall, London, 1-36.
- Manzi, V., Roveri, M., Gennari, R., Bertini, A., Biffi, U., Giunta, S., Iaccarino, S.M., Lanci, L., Lugli S., Negri, A., Riva, A., Rossi, M.E., Taviani, T., 2007. The deep-water counterpart of the Messinian Lower Evaporites in the Apennine foredeep: The Fanantello section (Northern Apennines, Italy). *Palaeogeography, palaeoclimatology, Palaeoecology* 251, 470-499.
- Martinsen, O., 1994. Mass movements. In: *The geological deformation of sediments* (1<sup>st</sup> edition). Chapman and Hall, London, 127-164.
- Mazumder, R., Van Loon, A.J., Arima, M., 2006. Soft sediment deformation structures in the Earth's oldest seismites. *Sedimentary Geology* 186, 19-26.

- McConnico, T.S., Bassett, K.N., 2007. Gravelly Gilbert-type fan delta on the Conway Coast, New Zealand: Foreset depositional processes and clast imbrications. *Sedimentary Geology* 198, 147-166.
- Meyn, H.D., Palonen P.A., 1980. Stratigraphy of an Archean submarine fan. *Precambrian Research* 12, 257-285.
- Milési, J., Ledru, P., Feybesse, J., Dommangeat, A., Marcoux, E., 1992. Early Proterozoic ore deposits and tectonics of Birimian orogenic belt, West Africa. *Precambrian Research* 58, 305- 344.
- Milési, J.P., Feybesse, J.L., Ledru, P., Dommangeat, A., Ouedraogo, M.F., Prost, A., Vinchon, C., Sylvain, J.P., Johan, V., Tegyey, M., Calvez, J.Y. Lagny, Ph., 1989. Les minéralisations aurifères de l'Afrique de l'Ouest. Leur évolution lithostructurale au Protérozoïque inférieur. *Chronicle. Recherché. Minière, France* 497, 3-98.
- Milési, J.P., Ledru, P., Ankrah, P., Johan, V., Marcoux, E., Vinchon, Ch., 1991. The metallogenetic relationship between Birimian and Tarkwaian gold deposits in Ghana. *Mineralium Deposita* 26, 228-238.
- Montenat, C., Barrier, P., d'Estevou, P.O., Hibsche, C., 2007. Seismites: An attempt at critical analysis and classification. *Sedimentary Geology* 196, 5-30.
- Naylor, M.A., 1981. Debris flow (olistostromes) and slumping on a distal passive continental margin: the Palombini limestone-shale sequence of the northern Apennines. *Sedimentology* 28, 837-852.
- Nemec, W., 1990. Aspects of sediment movement on steep delta slopes. Special Publication of the International Association of Sedimentologists 10, 29-73.
- Oberthür, T., Vetter, U., Davis, D.W., Amanor, J.A., 1998. Age constraints on gold mineralization and Paleoproterozoic crustal evolution in the Ashanti belt of southern Ghana. *Precambrian Research* 89, 129-143.
- Paciullo, F.V.P., Ribeiro, A., Trouw, R.A.J., Passchier, C.W., 2007. Facies and facies association of the siliciclastic Brak River and carbonate Gemsbok formation in the Lower Ugab River valley, Namibia, W. Africa. *Journal of Earth Sciences* 47, 121-134.
- Pawlak, S., Gueye, M., Klischies, R., Schwarz, S., Wemmer, K., Siegesmund, S. 2006. Geochemical and Sr-Nd isotopic data on the Birimian of the Kedougou-Kéniéba Inlier (Eastern Senegal): Implications on the Palaeoproterozoic evolution of the West African Craton. *South African Journal of Geology* 109, 411-427.
- Pierre C., Caruso, A., Blanc-Valleron, M., Rouchy, J.M., Orzsaq-Sperber, F., 2006. Reconstruction of the paleoenvironment changes around the Miocene-Pliocene boundary along a West-East transect across the Mediterranean. *Sedimentary Geology* 188-189, 319-340.

- Ponce, J.J., Olivero, E.B., Martinioni, D.R., 2008. Upper Oligocene-Miocene clinoforms of the foreland Austral Basin of Tierra del Fuego, Argentina: Stratigraphy, depositional sequences and architecture of the foredeep deposits. *Journal of South American Earth Sciences* 26, 36-54.
- Pons, J., Barbey, P., Dupuis, D., Leger, J.M., 1995. Mechanisms of pluton emplacement and structural evolution of a 2.1 Ga juvenile continental crust: the Birimian of South Western Niger. *Precambrian Research* 70, 281-301.
- Proyer, A., Mposkos, E., Baziotis, I., Hoinkes, G., 2008 Tracing high-pressure metamorphism in marbles: Phase relation in high grade aluminous calcite-dolomite marbles from the Greek Rhodope massif in the system CaO-MgO-Al<sub>2</sub>O<sub>3</sub>-SiO<sub>2</sub>-CO<sub>2</sub> and indications of prior aragonite. *Lithos* 104: 119-130.
- Queaño, K.L., 2005. Upper Miocene to Lower Pliocene Formation turbidites, on the Pujada Peninsula, Mindanao, Philippines: internal structures, composition, depositional elements and reservoir characteristics. *Journal of African Earth Sciences* 25, 387-402.
- Robins, P.S., 2006. The quantification of grade uncertainty, and associated risk, and their influence on pit optimization for the Sadiola Deep sulphide prefeasibility project. MSc thesis, University of the Witwatersrand, Johannesburg, pp.1-139.
- Schröder, S., Grotzinger, J.P., Amthor, J.E., Matter, A., 2006. Carbonate deposition and hydrocarbon reservoir development at the Precambrian-Cambrian boundary: The Ara group in South Oman. *Sedimentary Geology* 180, 1-28.
- Schwartz, M.O., Melcher, F., 2004. The Faleme Iron district, Senegal. Economic geology and the Bulletin of the Society of Economic Geologists 99, 919-939.
- Sestini, G., 1970. Flysch facies and turbidite sedimentology. *Sedimentary Geology* 4, 559-597.
- Shanmugam, G., 1997. The Bouma Sequence and the turbidite mind set. *Earth Science Reviews* 42, 201-229.
- Shanmugam, G., 2000. 50 years of the turbidite paradigm (1950s-1990s): deep water processes and facies models- a critical perspective. *Marine and Petroleum Geology* 17, 285-342.
- Shanmugam, G., Moiola, R.J., McPherson, J.G., O'Connell, 1988. Comparison of turbidite facies association in modern passive-margin Mississippi fan with active margin fans. *Sedimentary Geology* 58, 63-77.
- Stow, A.V., Johansson, M., 2000. Deep-water massive sands: nature, origin and hydrocarbon implications. *Marine and Petroleum Geology* 17, 145-174.
- Stow, D.A.V., 1986. Deep clastic seas. In: *Sedimentary Environments and Facies*, 2<sup>nd</sup> edition (ed. H.G. Reading). Blackwell Scientific Publications, Oxford, 399-444.

- Stromberg, S.G., Bluck, B., 1998. Turbidite facies, fluid-escape structures and mechanisms of emplacement of the Oligo-Miocene Aljibe Flysch, Gibraltar Arc, Betics, southern Spain. *Sedimentary Geology* 115, 267-288.
- Taylor, P.N., Moorbathe, S., Leube, A., Hirdes, W. 1992. Early Proterozoic crustal evolution in the Birimian of Ghana: Constraints from geochronology and isotope geochemistry. *Precambrian Research* 56, 97-111.
- Thiéblemont, D., Goujou, J.C., Egal E., Cocherie, A., Delor, C., Lafon, J.M., Fanning M. 2004. Archaean Evolution of the Leo Rise and its Eburnean reworking. *Journal of African Earth Sciences* 39, 97-104.
- Tshibubudze, A., 2007. Relative timing of structural events: the Markoye fault and its association to gold mineralisation. Honours thesis, University of the Witwatersrand, Johannesburg, 78p.
- Verplanck P.L., Mueller S.H., Goldfarb R.J., Nordstrom D.K., Youcha E.K., (2008). Geochemical controls of elevated arsenic concentrations in groundwater, Ester Dome. *Chemical Geology*, 255: 160-172
- Watkins, A.P., Liffe, J.E., Sharp, W.E., 1993. The effects of extensional and transpressional tectonics upon the development of Birimian sedimentary facies in Ghana, West Africa: Evidence from the Bomfa/Beposo District, near Konongo. *Journal Africa Earth Science*
- Yuguchi, T., Nishiyama, T., 2007. Cooling process of a granitic body deduced from the extents of exsolution and deuteric sub-solidus reactions: Case study of the Okueyama granitic body, Kyushu, Japan. *Lithos* 97, 395-421.
- US Department of State, 2008. Background Note: Mali, Bureau of African Affairs, October 2008.

## Appendix

### Petrography

#### Sample DFE3-046-002

Location: FE3 pit 1, core-log DFE3-046

Rock type: quartzite

The quartzite sample consists mainly of recrystallized quartz. The rock sample is very fine grained.

The sample consists of interlocked grains and this is interpreted as an indication of metamorphism.

#### Sample DFE3-046-003

Location: FE3 pit 1, core-log DFE3-046

Rock type: quartzite

The rock sample consists mainly of recrystallized quartz grains. The quartzite is very fine grained with a pinkish potassium feldspar staining. The potassium staining is interpreted as an indication of a contact aureole around the rocks.

#### Sample DFE3-046-004

Location: FE3 pit 1, core-log DFE3-046

Rock type: Breccia

The breccia is composed of quartz clasts embedded in an iron-oxide matrix. The clasts display a variety of shapes, from angular to sub-rounded. The clasts are medium grained. The breccia contains arsenopyrite.

#### Sample DFE3-046-005

Location: FE3 pit 1, core-log DFE3-046

Rock type: Marble

The marble is composed of recrystallized calcite and quartz grains. The rock sample is very fine grained. The calcite grains make up to 80% of the rock and the quartz grains mostly occur as quartz veins cross-cutting the calcite host rock. This has been interpreted as an indication of silicification in the marble.

#### Sample DFE3-046-006

Location: FE3 pit 1, core-log DFE3-046

Rock type: Marble

The marble is composed of recrystallised calcite and quartz. The calcite grains are relatively larger and have a 120° cleavage. The calcite host rock is cross-cut by quartz veins and this is interpreted as an indication of silicification of the marble. The rock sample is very fine grained.

#### Sample DFE3-047-008

Location: FE3 pit 1, core-log DFE3-047

Rock type: Iron oxide breccia

The breccia is composed of quartz grains in an iron-oxide matrix. The matrix makes almost 60% of the rock and consists of goethite and hematite. The quartz grains are medium grained and consists of various shapes ranging from angular to sub-rounded.

#### Sample DFE3-047-011

Location: FE3 pit 1, core-log DFE3-047

Rock type: Marble

The marble is composed of recrystallised calcite and quartz grains. The rock sample is very fine grained.

#### Sample SDFE3-003-025

Location: FE3 pit 1, core-log DFE3-003

Rock type: Breccia

The breccia is composed of clasts of calcite in a sulphide-rich iron oxide matrix. The sulphides include arsenopyrite and pyrite. The clasts are medium grained and consists of various shaped-calcite. The breccia is skorodite-rich. Skorodite is an alteration product of arsenopyrite.

#### Sample 270

Location: FE3 pit 1, GPS coordinates: 1535871; 0215824

Rock type: Greywacke

The greywacke sample is composed almost entirely of quartz. The rock sample consists of angular-shaped of quartz grains in a finer-grained quartz matrix. The matrix makes up to 30% of the rock. The quartz grains vary in diameter from 0.1mm to 5mm.

#### Sample 022

Location: FE3 pit 1, GPS coordinates: 1535853; 0215795

Rock type: Breccia

The breccias are composed of calcite clasts in an iron-oxide matrix. The calcite clasts are mostly angular in shape and are medium grained. The matrix contains hematite and goethite.

#### Sample 107

Location: FE3 pit 3, GPS coordinates: 1534432; 0216688

Rock type: Quartzite

The quartzite is composed almost entirely of recrystallised quartz. The rock also contains some calcite grains but these are very few. The rock is very fine grained and has no matrix.

#### Sample 40

Location: FE3 pit 1

Rock type: Iron oxide

This sample is composed of grains of hematite and goethite. In hand-specimen this is a laterite sample. There is zoning around the edges of the goethite.

#### Sample 202

Location: FE3 pit 2, GPS coordinates: 1534432; 0216688

Rock type: Marble

The marble is composed of recrystallised calcite grains. The rock has been highly altered and the grain boundaries are not visible anymore. The marble is potassium-rich. This has been interpreted as a result of contact metamorphism around a contact aureole.

#### Sample 200

Location: FE3 pit 2, GPS coordinates: 1534683; 0210331

Rock type: Granodiorite

The granodiorite is composed of plagioclase, biotite, sericite, orthoclase, quartz, and microcline. The plagioclase is subhedral, orthoclase is euhedral, microcline and quartz are sub-hedral and the biotite is anhedral. Sericite is an alteration mineral. The sample has been altered and has deuteritic textures (Fig. 16). The sample has been highly altered. The rock sample is medium-crystalline.

- Modal percentage: Plagioclase 20%

|            |     |
|------------|-----|
| Biotite    | 2%  |
| Orthoclase | 20% |
| Quartz     | 20% |
| Microcline | 35% |
| Sericite   | 3%  |

#### Sample 195

Location: FE3 pit 2, GPS coordinates: 1534683; 0210331

Rock type: Granodiorite

The sample is composed of plagioclase, biotite, sericite, orthoclase, quartz, and microcline. The sample has sericite alteration (Fig. 15). The plagioclase is subhedral, orthoclase is euhedral, microcline and quartz are sub-hedral and the biotite is anhedral. Sericite is an alteration mineral. The sample has been highly altered. The rock sample is medium-crystalline.

- Modal percentage: Plagioclase 30%

|            |     |
|------------|-----|
| Biotite    | 2%  |
| Orthoclase | 25% |
| Quartz     | 15% |
| Microcline | 30% |
| Sericite   | 3%  |

#### Sample 190

Location: FE3 pit 2, GPS coordinates: 1534773; 0216309

Rock type: Quartzite

- Consists of recrystallised quartz.
- The rock sample is very fine grained.

#### Sample 210

Location: FE3 pit 2, GPS coordinates: 1534920; 0216334

Rock type: Marble

The marble is composed of calcite crystals. The rock sample is very fine grained. The rock sample has been altered. The sample contains potassium staining. This is interpreted as a result of contact metamorphism around a contact aureole.

#### Sample 211

Location: FE3 pit 2, GPS coordinates: 1534916; 0216352

Rock type: Marble

The marble is composed of very fine recrystallised calcite crystals.

#### Sample 285

Location: FE3 pit 3, GPS coordinates: 1534916; 0216352

Rock type: Iron oxide breccia.

The breccia is composed of angular grains of calcite and quartz in an iron-oxide matrix. The clasts are medium grained. The matrix makes up to 40% of the rock and consists of hematite and goethite.

#### Sample SDFE3-007-014

Location: FE3 pit 3, core-log SDFE3-007

Rock type: Iron oxide Breccia

The breccia is composed of brecciated grains of calcite and quartz in an iron oxide matrix.

The clasts are medium grained. The matrix consists of hematite and goethite.

#### Sample SDFE3-007-015

Location: FE3 pit 3, core-log SDFE3-007

Rock type: marble

The marble is composed of very fine recrystallised calcite grains. The sample is cross-cut by quartz veins and sulphide-rich veins. The rock contains octahedral-shaped pyrite grains.

#### Sample SDFE3-007-017

Location: FE3 pit 3, core-log SDFE3-007

Rock type: marble

The marble is composed of very fine recrystallised calcite. The rock contains microcline crystals.

Microcline is replaced by calcite.

Sample SDFE3-007-018

Location: FE3 pit 3, core-log SDFE3-007

Rock type: marble

The marble is composed of very fine recrystallised calcite.